Lens Aquaporin-5 Inserts Into Bovine Fiber Cell Plasma Membranes Via Unconventional Protein Secretion

Romell B. Gletten,[1] Lee S. Cantrell,[1] Sujoy Bhattacharya,[2] and Kevin L. Schey[1]

[1]Department of Biochemistry, Vanderbilt University, Nashville, Tennessee, United States
[2]Department of Ophthalmology and Visual Sciences, Vanderbilt University, Nashville, Tennessee, United States

Correspondence: Kevin L. Schey, Mass Spectrometry Research Center, Department of Biochemistry, 465 21st Avenue South, Suite 9160, Medical Research Building III, Vanderbilt University, Nashville, TN 37232-8575, USA; kevin.schey@vanderbilt.edu.

Received: February 14, 2022
Accepted: June 14, 2022
Published: July 11, 2022

Citation: Gletten RB, Cantrell LS, Bhattacharya S, Schey KL. Lens aquaporin-5 inserts into bovine fiber cell plasma membranes via unconventional protein secretion. *Invest Ophthalmol Vis Sci.* 2022;63(8):5. https://doi.org/10.1167/iovs.63.8.5

Purpose. To spatially map aquaporin-5 (AQP5) expression in the bovine lens, molecularly characterize cytoplasmic AQP5-containing vesicles in the outer cortex, and elucidate AQP5 membrane trafficking mechanisms.

Methods. Immunofluorescence was performed on bovine lens cryosections using AQP5, TOMM20, COX IV, calnexin, LC3B, Sec22β, LIMP-2, and connexin 50 antibodies and the membrane dye CM-DiI. AQP5 plasma membrane insertion was defined via line expression profile analysis. Transmission electron microscopy (TEM) was performed on bovine lens sections to examine cytoplasmic organelle morphology and subcellular localization in cortical fiber cells. Bovine lenses were treated with 10-nM bafilomycin A1 or 0.1% dimethyl sulfoxide vehicle control for 24 hours in ex vivo culture to determine changes in AQP5 plasma membrane expression.

Results. Immunofluorescence analysis revealed cytoplasmic AQP5 expression in lens epithelial cells and differentiating fiber cells. In the lens cortex, complete AQP5 plasma membrane insertion occurs at $r/a = 0.951 \pm 0.005$. AQP5-containing cytoplasmic vesicles are spheroidal in morphology with linear extensions, express TOMM20, and contain LC3B and LIMP-2, but not Sec22β, as fiber cells mature. TEM analysis revealed complex vesicular assemblies with congruent subcellular localization to AQP5-containing cytoplasmic vesicles. AQP5-containing cytoplasmic vesicles appear to dock with the plasma membrane. Bafilomycin A1 treatment reduced AQP5 plasma membrane expression by 27%.

Conclusions. AQP5 localizes to spheroidal, linear cytoplasmic vesicles in the differentiating bovine lens fiber cells. During fiber cell differentiation, these vesicles incorporate LC3B and presumably fuse with LIMP-2–positive lysosomes. Our data suggest that AQP5 to the plasma membrane through lysosome-associated unconventional protein secretion, a novel mechanism of AQP5 trafficking.

Keywords: AQP5, trafficking, autophagosome, amphisome, lysosome, lens fiber cells, mitochondria, autophagy

The ocular lens is a transparent, biconvex tissue in the eye that adjustably refracts visible light onto the retina, enabling high-acuity vision over a wide range of distances.[1–3] The optical properties of the lens are a function of its specialized cellular organization, which is comprised of an anterior monolayer of epithelial cells that overlay and differentiate into lens fiber cells at the lens equator.[4] Fiber cells differentiate gradually through a process of protein synthesis, cell migration, cell elongation, and programmed organelle degradation to form a gradient of cellular differentiation and spatiotemporal protein expression from the lens periphery to the lens core.

Aquaporins (AQPs) are transmembrane water channels that represent one group of spatiotemporally expressed proteins in the lens. Mammalian lenses express AQP0,[5–8] AQP1,[8,9] and AQP5.[8,10–12] Collectively, lens AQPs regulate lens transparency and refractive index[13] by controlling lens osmotic balance. In lens epithelial cells, AQP1 is expressed on the apical plasma membrane,[14,15] and AQP5 is expressed cytoplasmically.[15–17] In lens fiber cells, AQP0 is expressed on the apical and basolateral plasma membranes while AQP5 is cytoplasmically expressed in the newly differentiating fiber cells and is gradually inserted into the plasma membrane as fiber cells mature.[12,15–17]

The important role of AQP5 in maintaining lens homeostasis is implied by its expression in all mammalian lenses studied to date including human,[12,18–20] bovine,[12] mouse,[11,12,16,17,19–21] rat,[12,17,21] rabbit,[8] and dog[22] lenses. Functional studies have demonstrated the relationship between AQP5 expression and lens osmotic homeostasis. For example, basal water content and volume are increased by ~22% and 12%, respectively, in AQP5 knockout ($AQP5^{-/-}$) mouse lenses relative to wild-type ($AQP5^{+/+}$) lenses following osmotic perturbation in hyperglycemic media.[23,24] $AQP5^{-/-}$ mouse lenses develop cataract under the same conditions but remain transparent[14,23] following normoglycemic culture, in contrast to $AQP5^{+/+}$ and $AQP0^{-/-}$ mice.[25–29] $AQP5^{-/-}$ mice also develop age-related cataract

Investigative Ophthalmology & Visual Science

around 6 months at a higher frequency than AQP5$^{+/+}$ mice through upregulation of vimentin expression via miR-124–3p.1 expression.[20] The same effect is achieved in mice with a leucine to proline missense mutation at residue 51 in AQP5, AQP5^{L51P}, which corresponds to a homologous mutation in humans (*h*AQP5^{L51P}) associated with congenital cataract.[20]

Functional studies have also demonstrated the relationship between AQP5 subcellular localization and fiber cell plasma membrane water permeability (P_{H2O}) in the lens. Immunohistochemical studies have shown that AQP5 primarily localizes to the plasma membrane in the fiber cells of the mouse lens cortex and to cytoplasmic vesicles in the rat lens cortex, and the extent of fiber cell permeability correlates to plasma membrane AQP5 abundance.[17] Cytoplasmic AQP5 in rat lenses is dynamically inserted into fiber cell plasma membranes in response to changes in zonular tension and thereby increases fiber cell plasma membrane water permeability (P_{H2O}).[17,21]

Although the expression and functional regulation of lenticular AQP5 are currently being investigated, the molecular identity of lens AQP5-containing cytoplasmic vesicles remains unclear. AQP5 has been shown to localize to autophagosomes for degradation in both mouse and rat submandibular glands.[30,31] In this study, we spatially mapped AQP5 in the bovine lens, defined the molecular identity of AQP5-containing cytoplasmic compartments, and investigated mechanisms of AQP5 plasma membrane insertion. In the bovine lens, we found that AQP5 is expressed cytoplasmically in the lens epithelial and outer cortical fiber cells and then is gradually inserted into fiber cell plasma membranes in the inner cortex, similar to other mammalian lenses. Based on our immunofluorescence analysis in the outer cortex, AQP5 appears to be associated with and possibly incorporated into mitochondria in the bovine lens. Thereafter, AQP5-containing cytoplasmic vesicles are identified as microtubule-associated protein 1 light chain 3B (LC3B)-positive, lysosomal integral membrane protein 2 (LIMP-2)-positive vesicles in which TOMM20-containing mitochondria appear to degrade, possibly as a specialized method of normal lens mitochondrial autophagic degradation. These AQP5-containing cytoplasmic vesicles appear to dock with the plasma membrane with subsequent AQP5 plasma membrane insertion. AQP5 plasma membrane expression is decreased by bafilomycin A1 treatment, suggesting a novel type of AQP5 trafficking through lysosome secretion, a form of type III unconventional protein secretion, in the mammalian cells.

Materials and Methods

Tissue

Fresh bovine lenses (1–2 years old) used for immunofluorescence were obtained from Light Hill Meats (Lynnville, TN, USA) and Cedar Hill Meat Processing (Cedar Hill, TN, USA).

Reagents

All chemicals, unless otherwise stated, were obtained from Sigma-Aldrich (St. Louis, MO, USA). Bafilomycin A1 was purchased from MilliporeSigma (Burlington, MA, USA).

Antibodies

Affinity-purified rabbit anti-AQP5 IgG antibody targeted toward amino acid residues 249 to 265 of rat AQP5 (AB15858) and normal goat IgG antibody (NI02-100UG) were obtained from MilliporeSigma. Normal rabbit IgG antibodies (2729) were obtained from Cell Signaling Technology (Danvers, MA, USA). Goat anti-calnexin IgG (LS-B4403) was obtained from LifeSpan BioSciences (Dallas, TX, USA). Rabbit anti-LC3B IgG (MBS9435173) was obtained from MyBioSource (San Diego, CA, USA). Rabbit anti-LIMP-2 IgG (NB400-129) was obtained from Novus Biologicals (Centennial, CO, USA). Mouse anti-TOMM20 IgG (ab56783) was obtained from Abcam (Waltham, MA, USA). Goat anti-connexin 50 IgG (sc-20746) and normal mouse IgG (sc-2025) antibody were obtained from Santa Cruz Biotechnology (Dallas, TX, USA). Secondary antibodies (goat anti-rabbit Alexa Fluor 488, goat anti-rabbit Alexa Fluor 647, donkey anti-rabbit Alexa Fluor 488, and donkey anti-goat Alexa Fluor 647) were obtained from Thermo Fisher Scientific (Waltham, MA, USA). Secondary antibody used for western blotting (goat anti-rabbit DyLight 680, goat anti-mouse DyLight 800, and donkey anti-goat DyLight 800) was obtained from Thermo Fisher Scientific.

Other Biologics

Alexa Fluor 488- or Alexa Fluor 647-conjugated wheat germ agglutinin (WGA) was used to label fiber cell plasma membranes. Invitrogen Vybrant CM-DiI Cell-Labeling Solution (V22888; Thermo Fisher Scientific) was used to universally label lipid membranes in fiber cells.

Immunofluorescence

Fresh or cultured bovine lenses were fixed in 2% paraformaldehyde with or without 0.01% glutaraldehyde in phosphate buffered saline (PBS) for 72 hours at room temperature and then cryoprotected in 10% sucrose–PBS for 2 days at 4°C; 20% sucrose–PBS for 1 hour at room temperature; and 30% sucrose–PBS for ≥7 days at 4°C. They were then snap frozen in liquid nitrogen, encased in Tissue-Tek O.C.T. Compound (Sakura Finetek USA, Torrance, CA, USA), and cryosectioned parallel (axially) to the optic axis at 20-µm thickness using a Leica CM3050 S Research Cryostat (Leica Biosystems, Buffalo Grove, IL, USA). Finally, they were transferred onto plain microscope slides. Next, lens tissue cryosections (i.e., "sections") were triply washed in PBS, incubated in blocking solution (6% bovine serum albumin and 6% normal goat serum in PBS) for 2 to 3 hours to reduce nonspecific labeling, and then immunolabeled with rabbit anti-AQP5 (1:400), goat anti-calnexin (1:100), mouse anti-TOMM20 (1:200), rabbit anti-LC3B (1:400), rabbit anti-Sec22β (1:100), or rabbit anti-LIMP2 (1:250) primary antibody in blocking solution for 16 hours at 4°C, followed by Alexa 488- or Alexa 647-conjugated goat or donkey secondary antibodies in blocking solution for 2 hours at room temperature.

Normal rabbit IgG, normal goat IgG, and normal mouse IgG were used as host-specific negative controls for nonspecific IgG binding. In certain cases, 0.1% Triton X-100 was included in PBS washes or blocking solution prior to incubation with secondary antibodies. Following immunolabeling, sections underwent subsequent fluorescent labeling with 4′,6-diamidino-2-phenylindole (DAPI)–dilactate

Investigative Ophthalmology & Visual Science

(1:100 in PBS) to label cellular nuclei singularly or DAPI–dilactate in combination with Alexa 488- or Alexa 647-conjugated WGA (1:100 in PBS) for 1 hour at room temperature to label fiber cell plasma membranes or Vybrant CM-DiI Cell-Labeling Solution Lipid (1:5000 in 50% ethanol–PBS) to label cellular lipid membranes. Following immunolabeling and labeling, sections were coverslipped in Invitrogen ProLong Glass Antifade Mountant (Thermo Fisher Scientific) and imaged using a Zeiss LSM 880 confocal laser scanning microscope (Carl Zeiss, Inc., White Plains, NY, USA). Images were postprocessed to improve resolution using Airyscan processing (Zeiss). Background fluorescence (i.e., fluorescence from normal IgG-incubated, negative control tissue) was subtracted using Photoshop CS6 (Adobe; San Jose, CA, USA).

Ex Vivo Whole Lens Culture and Image Segmentation Analysis

Fresh bovine lenses were cultured in complete medium at 37°C in 4% CO_2 as outlined previously[32] using a Thermo Forma Model 370 Series Steri-Cycle CO_2 Incubator (Thermo Fisher Scientific). Briefly, complete M199 medium consisted of M199 medium (11-150-059; Thermo Fisher Scientific), 10% fetal bovine serum, 1% penicillin, and 1% streptomycin. After 2 hours of culture, lenses free of cataract were treated with 10-nM bafilomycin A1 or 0.1% dimethyl sulfoxide (DMSO), the vehicle (negative) control, for 24 hours. Cultured bovine lenses were cryosectioned for immunofluorescence analysis and imaged as outlined above. NIS-Elements 5.3.0 software (Nikon, Tokyo, Japan) was used to perform image segmentation to quantify relative AQP5 expression changes in the cortical fiber cell plasma membranes of cultured bovine lenses due to bafilomycin A1 treatment. Relative AQP5 expression was defined as the mean intensity of AQP5 immunofluorescence with bafilomycin A1 treatment normalized to vehicle control.

Transmission Electron Microscopy

Fresh bovine lenses were placed in 1% glutaraldehyde in 0.1-M cacodylate buffer for 2 days at room temperature. Thereafter, tissue chunks were excised from these lenses near the lens equator and incubated in 2.5% glutaraldehyde–0.1-M cacodylate for 2 days at room temperature, followed by post-fixation in 1% OsO_4 for 1 hour at room temperature. The tissue was dehydrated using a graded ethanol series and infiltrated with Epon-812 (RT 13940; Electron Microscopy Sciences, Hatfield, PA, USA) using propylene oxide as the transition solvent. The Epon-812 was polymerized at 60°C for 48 hours, and the samples were sectioned at 70 nm for transmission electron microscopy (TEM) using a Leica UC7 Ultramicrotome (Leica Microsystems, Wetzlar, Germany). TEM was performed on a Tecnai T12 electron microscope (Thermo Fisher Scientific) at 100 kV using a charge-coupled device camera (Advanced Microscopy Techniques, Woburn, MA, USA).

Lens Homogenization and Liquid Chromatography With Tandem Mass Spectrometry for Identifying LIMP-2 Peptides

Frozen bovine lens anterior and posterior poles were shaved off to yield a center section approximately 3 mm thick. The cortex was removed by trephine center-punch at 7/16 inch and homogenized in homogenizing buffer (25-mM Tris, 5-mM EDTA, 1-mM dithiothreitol, 150-mM NaCl, 1-mM phenylmethylsulfonyl fluoride, pH 8.0), then centrifuged at 100,000*g* for 30 minutes to pellet the membrane fraction. The membrane fraction was subsequently washed in homogenizing buffer once, homogenizing buffer with 8-M urea twice, then cold 0.1-M NaOH. Urea-insoluble/NaOH-insoluble membrane fraction proteins were taken up in 50-mM triethylammonium bicarbonate (TEAB) and 5% SDS, and 75 µg protein was isolated. The protein isolate was reduced and alkylated with addition of 10-mM dithiothreitol and 20-mM iodoacetamide. Alkylated proteins were acidified with phosphoric acid to 2.5% and precipitated with 100-mM TEAB in methanol. Precipitate was loaded on an S-Trap micro kit (ProtiFi, Farmingdale, NY, USA), washed four times with 100-mM TEAB in methanol, and digested in 0.25-µg/µL trypsin in 50-mM TEAB for 2 hours at 46°C.

Peptides were eluted from the S-Trap with 66-mM TEAB, 0.2% formic acid, and then 66-mM TEAB and 50% acetonitrile (ACN). Eluted peptides were dried by a SpeedVac vacuum concentrator (Thermo Fisher Scientific) and rehydrated in 0.1 % triethylamine (TEA). Peptides were basic reverse phase separated on an in-house fabricated STAGE tip. Briefly, two 1.0-mm Empore C18 filter plugs were added to a pipette tip, and 2 mg 5-µm C18 resin (Phenomenex, Torrance, CA, USA) was added to the top of the C18 filter plug. Peptides were loaded to the stage tip after equilibration and washed twice in 0.1% TEA. Peptides were eluted from the STAGE tip in progressive fractions of ACN (5%, 7.5%, 10%, 12.5%, 15%, 20%, 30%, 50% in 0.1% TEA). Dried fractions were reconstituted in 0.1% formic acid. Approximately 400 ng of each basic reverse-phase fraction was separately loaded onto a trap column before separation along a 95-minute gradient from 5% to 37% ACN.

Peptides were measured on a Velos Pro Linear Ion Trap Mass Spectrometer (Thermo Fisher Scientific) operating in Top15 data-dependent tandem mass spectrometry acquisition mode. RAW files were searched with FragPipe 17.0 and modified to accommodate the low-resolution mass analyzer used in this study. Briefly, each sample was selected as part of a single experiment and searched with MSFragger 3.4 with precursor mass tolerance of ±500 ppm and fragment mass tolerance of ±0.7 Da. Peptides of length 7 to 50 in mass range 500 to 5000 with charge 1 to 4 were included in a database of reviewed and unreviewed proteins (downloaded December 8, 2016; length 32,167). Cysteine carbamidomethylation was included as a default modification. Up to two variable modifications of methionine oxidation and N-terminal excision were allowed per peptide. Protein level results were filtered at a 5% false discovery rate (FDR), and peptides, peptide spectrum matches, and ions were filtered at a 1% FDR. FragPipe outputs were used for protein-level data interpretation in R (R Foundation for Statistical Computing, Vienna, Austria).

Statistical Analysis

All assays were conducted in at least triplicate, and experimental results are represented as the data mean ± standard error of the mean. The statistical significance of the experimental results was determined with Student's *t*-test. $P \leq 0.05$ was considered statistically significant.

Investigative Ophthalmology & Visual Science

Results

AQP5 has been spatially mapped in human,[12] mouse,[12,15,16] rat,[12,21] and rabbit[8] lenses. AQP5 spatial expression is broadly consistent across these species. AQP5 is cytoplasmic in lens epithelial cells and in young, differentiating fiber cells of the lens cortex; as fiber cells mature, it is gradually inserted into fiber cell plasma membranes. AQP5 expression remains localized to the plasma membrane in mature fiber cells to the lens core.

AQP5 Localization and Membrane Insertion

Based on these findings, we hypothesized that this general AQP5 spatial expression pattern is characteristic of mammalian lenses and would also be observed in bovine lenses. Confocal microscopy analysis of bovine lens cryosections immunolabeled for AQP5 shows that AQP5 is expressed throughout the bovine lens in both lens epithelial cells and lens fiber cells (Figs. 1A, 1B). AQP5 expression is cytoplasmic in bovine lens epithelial cells and in the incipient fiber cells of the lens modiolus (Figs. 1C, 1D). Interestingly, nuclear AQP5 expression consistently becomes detectable in the peripheral outer cortex immediately after fiber cells exit the lens modiolus and undergo substantial elongation (Figs. 1C, 1D, closed arrows). AQP5 plasma membrane insertion, defined as colocalization between AQP5 immunolabeling and WGA labeling, is detectable alongside cytoplasmic AQP5 expression as differentiating cortical fiber cells mature (Figs. 1E, 1F, arrowheads). AQP5 expression is completely localized to the plasma membrane in the inner cortex and remains integral to the membrane through to the lens core. AQP5 nuclear expression disappears as AQP5 is inserted into the plasma membrane in the inner cortex (Figs. 1E, 1F, open arrows). AQP5 nuclear expression in the bovine lens appears to coincide with a reduction in cortical fiber cell nuclear size and change in morphology from smooth and elliptical in the outer cortex to irregular and elliptical in the inner cortex (Figs. 1C–1F).

AQP5 plasma membrane insertion was quantified based on the normalized radial distance r/a, where r is the radial distance to the lens center, and a is the lens radius,[33] as was done for previous mammalian lenses.[12] The fluorescence intensities of AQP5 and WGA in Figure 1 were converted to gray values (Figs. 2A, 2B), and collinear surface plots of these gray values as a function of r/a quantitatively depict the spatial relationship between AQP5 expression and the plasma membrane across the lens bow region (Figs. 2C–2E). AQP5 plasma membrane insertion is defined as r/a values with overlap between AQP5 and WGA gray values. AQP5 immunolabeling intensity peaks in the lens modiolus and decreases significantly with r/a in the outer cortical fiber cells. The surface plot data for cytoplasmic AQP5 immunolabeling is nonuniform, which reflects cytoplasmic AQP5 expression. Decreased AQP5 immunofluorescence intensity in the medial outer cortex may be a result of (1) reduced AQP5 local concentration due to fiber cell volumetric expansion during cellular elongation, (2) AQP5 C-terminal epitope masking, or (3) reduced AQP5 expression in this region, although this observation remains to be further studied. Initial AQP5 plasma membrane insertion is detectable from $r/a = 0.979$ (Figs. 2C, 2D, black star) to $r/a = 0.958$ (Figs. 2C, 2E, blue star). Cytoplasmic AQP5 immunolabeling is detected between these r/a values, as well. Full AQP5 membrane insertion occurs at $r/a = 0.958$ (blue star), which is in the outer cortex–inner cortex transitional region. AQP5 remains localized to the plasma membrane for $0.958 \geq r/a \geq 0.000$ (data not shown).

Identification of AQP5 Cytoplasmic Structures

Previous studies revealed variability in the morphology of AQP5-containing cytoplasmic vesicles in mouse,[12,16] rat,[12] and human[12] lens cortical fiber cells. To more accurately characterize AQP5-containing cytoplasmic vesicles in the bovine lens, we conducted high-resolution confocal microscopy imaging of AQP5 expression in bovine lens cortical fiber cells (Fig. 3). Cytoplasmic AQP5 expression in bovine lens fiber cells is localized to spheroidal cytoplasmic vesicles with linear components in the outer cortex (Fig. 3, arrowheads). As fiber cells begin to differentiate at the lens equator, AQP5-containing cytoplasmic vesicles are less than 1 µm in diameter, up to 20 µm in length, and predominantly linear in morphology (Fig. 3B, open arrowheads). As fiber cells mature and exit the lens modiolus, AQP5-containing cytoplasmic vesicles become predominantly spheroidal and spheroidal, linear (Fig. 3, closed arrowheads), with spheroid regions varying up to approximately 3.5 µm in diameter (Figs. 3C, 3D).

To test whether AQP5-containing cytoplasmic vesicles are morphologically distinct structures among cytoplasmic vesicles in bovine lens cortical fiber cells, we analyzed DiI-labeled, AQP5-immunolabeled bovine lens cryosections (Fig. 4). DiI is a lipophilic dye that labels all cytoplasmic cellular lipid membranes and the plasma membrane. In the lens modiolus, linear DiI-labeled cytoplasmic compartments overlap with linear, AQP5-containing cytoplasmic vesicles, indicating that these structures are morphologically unique (Fig. 4A, open arrowheads). In this region, DiI-labeled spheroidal, linear cytoplasmic compartments and AQP5-containing, cytoplasmic vesicles typically overlap, but such compartments lacking AQP5 expression are readily observable in this region (Fig. 4A, striped arrowheads). In outer cortical fiber cells, with the exception of the lens modiolus, spheroidal, linear DiI-labeled cytoplasmic compartments are identical to AQP5-containing, cytoplasmic vesicles with rare exceptions, indicating that large, spheroidal, linear cytoplasmic structures in the outer cortex are uniquely AQP5-containing cytoplasmic vesicles (Fig. 4, closed white arrowheads).

Immunohistochemical studies of mitochondria[34] in chick lens fiber cells revealed structures similar in morphology to AQP5-containing cytoplasmic vesicles. To determine the molecular composition of bovine lens fiber cell AQP5-containing cytoplasmic vesicles, we tested AQP5-containing cytoplasmic vesicles for the presence of mitochondrial import receptor subunit TOM20 homolog (TOMM20) (Fig. 5). TOMM20 is ubiquitously expressed in all linear (Fig. 5, open arrowheads) and spheroidal, linear (Fig. 5, closed arrowheads) AQP5-containing cytoplasmic vesicles observed. Colocalization between AQP5 and TOMM20 expression in these vesicles is high but not uniform throughout the entirety of structures. TOMM20 expression dissipates during full AQP5 plasma membrane insertion in the bovine lens fiber cells of the outer cortex–inner cortex transition zone (Fig. 5C). TOMM20 expression is not detected on the plasma membrane. The co-expression of AQP5 and TOMM20 in bovine lens cortical fiber cells indicates that TOMM20 is a molecular marker of AQP5-containing cytoplasmic vesicles. We also tested AQP5-containing

Investigative Ophthalmology & Visual Science

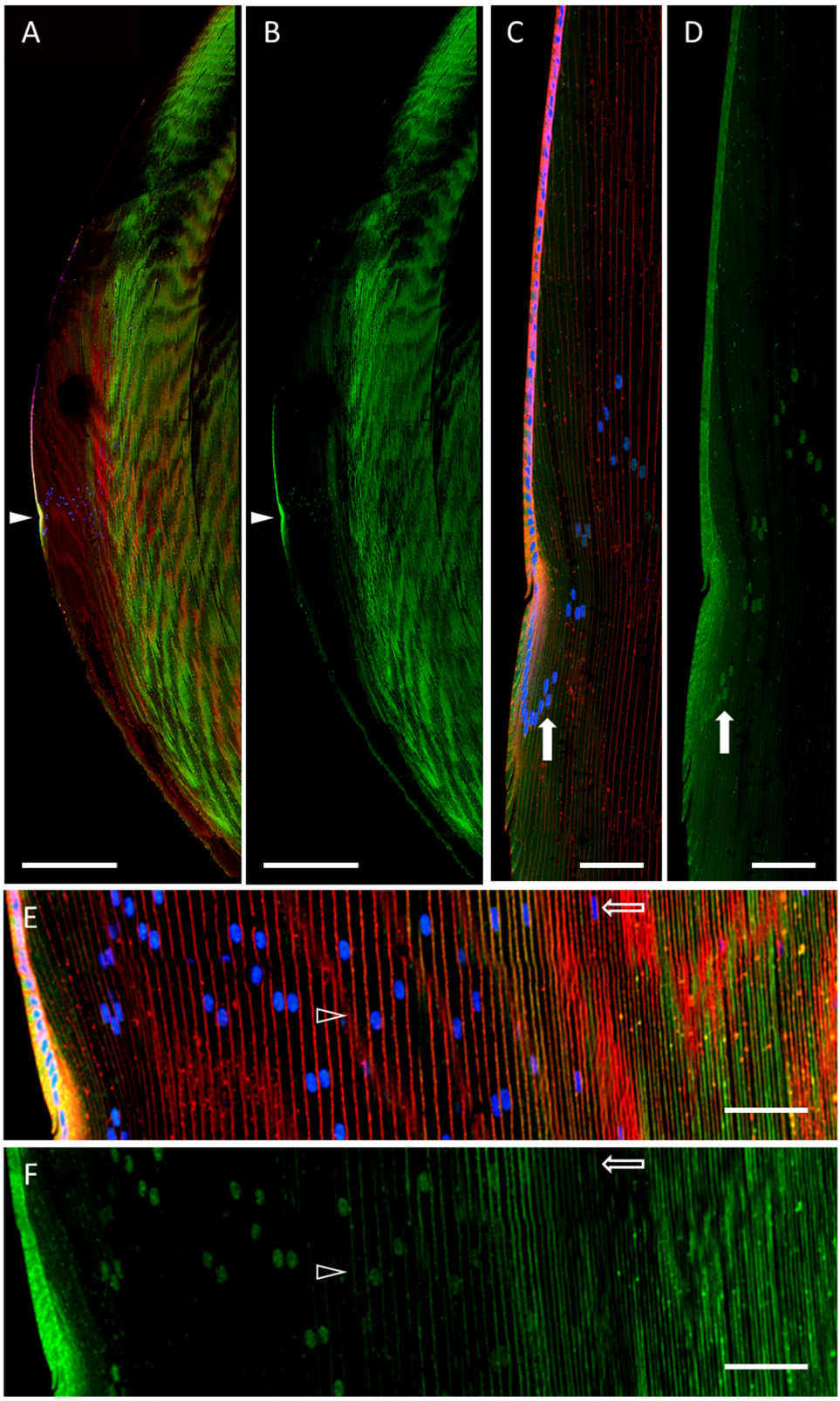

Figure 1. AQP5 spatial expression in the bovine lens. (**A**) A low-magnification, high-resolution image of AQP5 immunolabeling (*green*) in the bovine lens with WGA labeling of plasma membranes (*red*) and DAPI labeling of cell nuclei (*blue*). The *closed arrowhead* denotes the lens modiolus. (**B**) A replicate image of **A** with only AQP5 immunolabeling displayed. (**C**) A medium-magnification, high-resolution image of the lens modiolus and nearby outer cortical fiber cells. The *closed arrow* indicates the nucleus of an outer cortical fiber cell. (**D**) A replicate image of **C** with only AQP5 immunolabeling displayed. The *filled arrow* indicates AQP5 immunolabeling in the same cell nucleus shown in **B** and marks the appearance of AQP5 immunolabeling in outer cortical lens fiber cell nuclei. (**E**) A medium-magnification, high-resolution

Investigative Ophthalmology & Visual Science

image of the lens cortex. The *open arrowhead* indicates the appearance of AQP5 plasma membrane insertion. The *open arrow* indicates the nucleus of a differentiating cortical fiber cell. (**F**) A replicate image of **E** with only AQP5 immunolabeling displayed. *Scale bars*: 500 µm (**A**, **B**) and 100 µm (**C–F**). The *open arrow* indicates AQP5 immunolabeling in the same cell nucleus shown in **E** and marks the disappearance of AQP5 immunolabeling in inner cortical lens fiber cell nuclei.

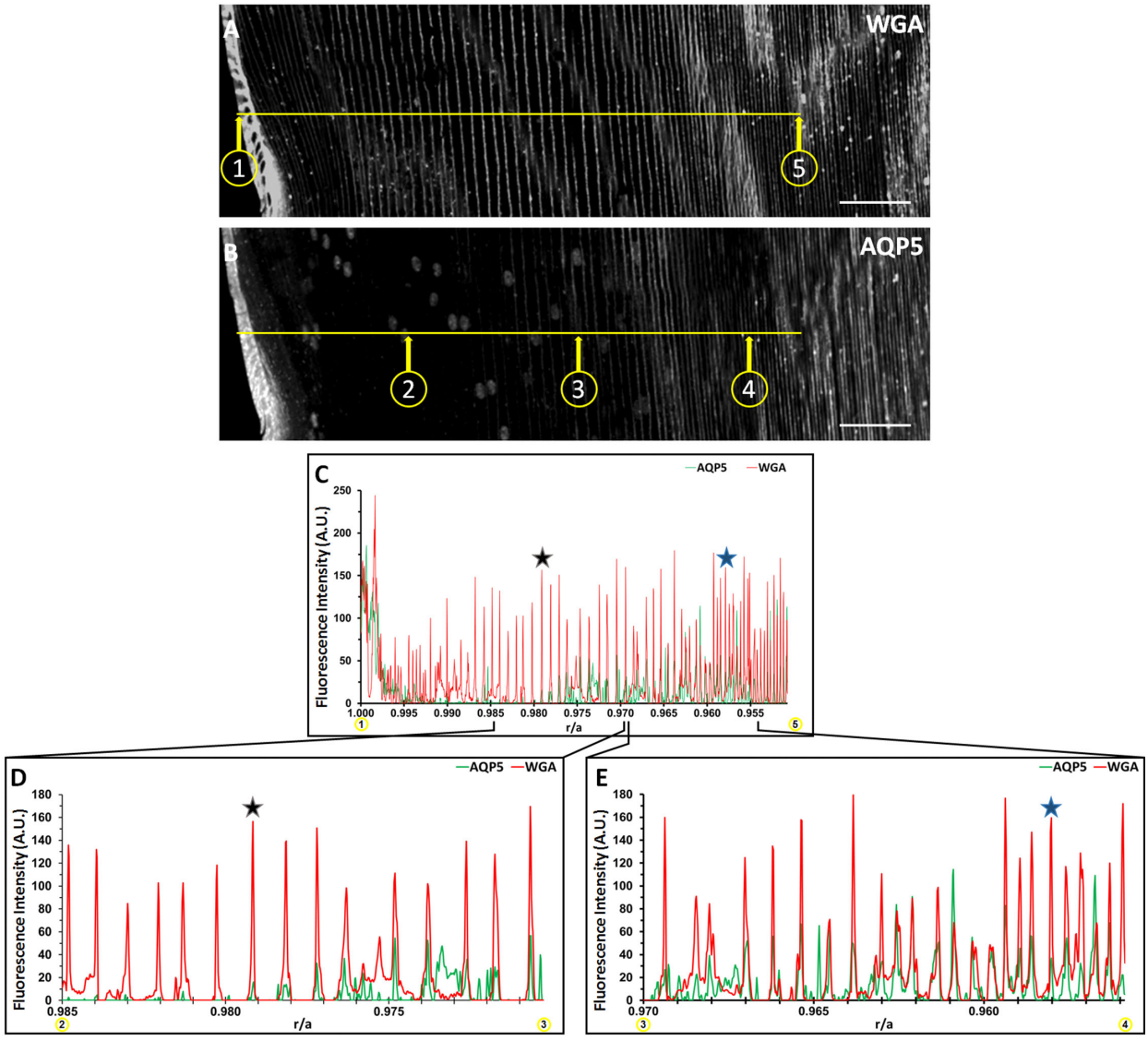

Figure 2. Cytoplasmic AQP5 is progressively inserted into cortical fiber plasma membranes during fiber cell differentiation in the bovine lens. (**A**) A grayscale image of Figure 1E with only WGA labeling displayed. Distinct points in space on a lens cryosection ($n = 1$) are represented by the quotient r/a, where r is the distance from any point to the center of the lens perpendicular to the optical axis, and a is the radius of the lens, which is 8000 µm for this section. *Circled point* 1 in **C** corresponds to $r/a = 1.000$, and *circled point* 5 corresponds to $r/a = 0.950$. The horizontal *yellow line* in **C** connects *circled points* 1 and 5. (**B**) A replicate, grayscale image of Figure 1E with only AQP5 immunolabeling displayed. The horizontal *yellow line* is collinear to the line in **B** and connects *circled points* 2, 3, and 4, which correspond to $r/a = 0.985$, $r/a = 0.970$, and $r/a = 0.955$, respectively. (**C**) Two-dimensional surface plots of the fluorescence-intensity gray values of WGA in **B** (*red line*) and AQP5 in **D** (*green line*) across the *yellow line* from *circled points* 1 to 5. (**D**) Two-dimensional surface plots of the fluorescence-intensity gray values of WGA in **B** (*red line*) and AQP5 in **D** (*green line*) across the *yellow line* from *circled points* 2 to 3. (**E**) Two-dimensional surface plots of the fluorescence intensity gray values of WGA in **B** (*red line*) and AQP5 in **D** (*green line*) across the yellow line from *circled points* 3 to 4. AQP5 fluorescence intensity maximizes at $r/a = 0.998$ then decreases rapidly to nearly undetectable levels at $r/a = 0.989$. AQP5 fluorescence intensity increases inversely with r/a and is partially overlapped in space by the fluorescence intensity of WGA from 0.979 (*black star*) $\geq r/a \geq$ 0.958 (*blue star*) (**D**, **E**) AQP5 fluorescence intensity is entirely overlapped by that of WGA in space at $r/a = 0.958$ (*blue star*) (**D**). This trend continues to the lens center ($0.958 \geq r/a \geq 0.000$; data not shown). *Scale bars*: 100 µm (**A**, **B**).

cytoplasmic vesicles for the presence of cytochrome c oxidase subunit IV (COX IV) (Supplementary Fig. S1), an inner mitochondrial membrane protein, and resident endoplasmic reticulum protein calnexin (Supplementary Fig. S2).

Investigative Ophthalmology & Visual Science

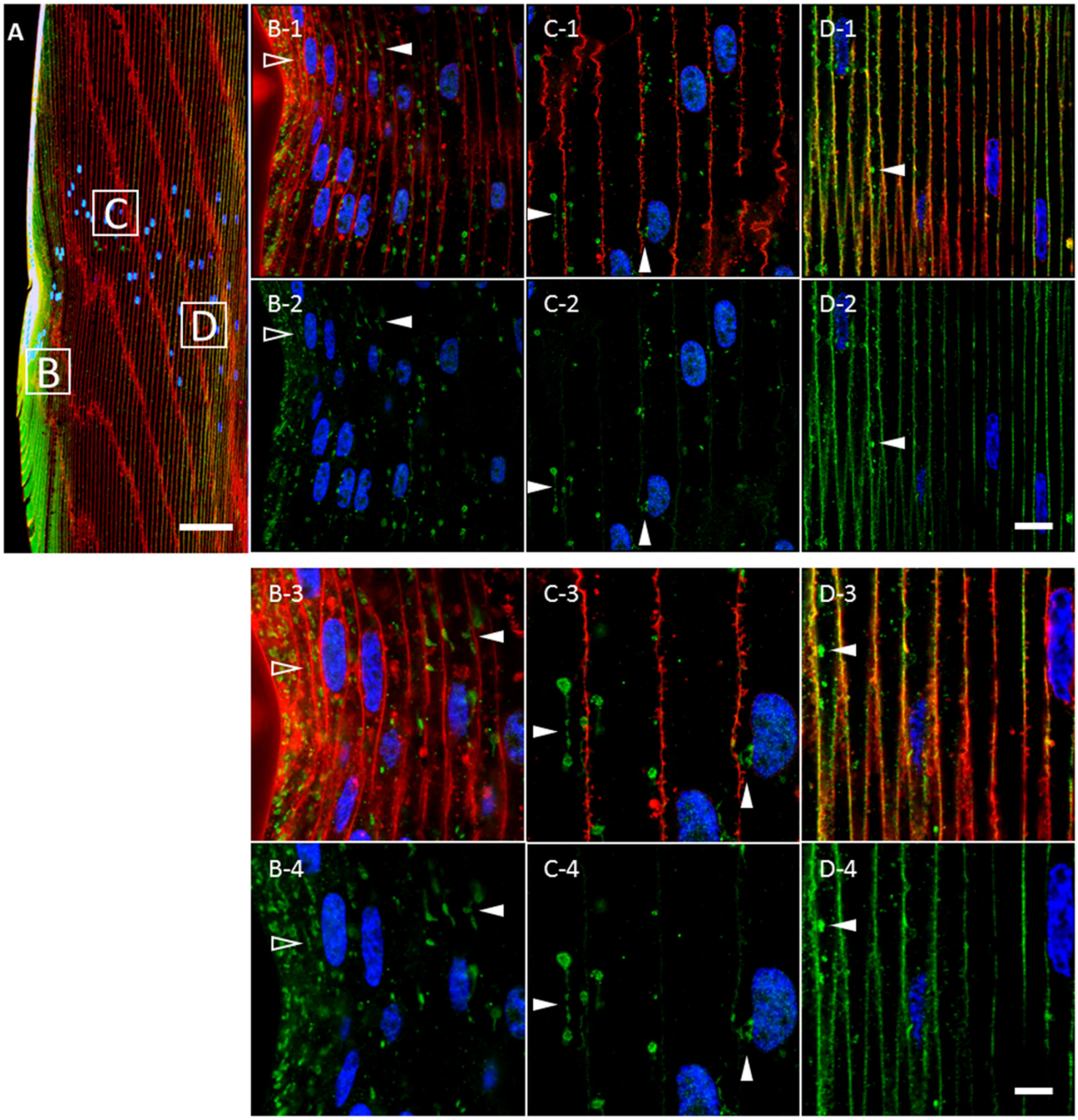

Figure 3. Cytoplasmic AQP5 immunolabeling in cortical fiber cells is localized to spheroidal, linear structures in the bovine lens bow region. (**A**) A low-magnification representative image of AQP5 immunolabeling (*green*) in the bovine lens bow region. Plasma membranes (*red*) and cellular nuclei (*blue*) are labeled by WGA and DAPI, respectively. The peripheral outer cortex (i.e., includes lens modiolus), medial outer cortex, and outer cortex–inner cortex transitional region are indicated by the *B*, *C*, and *D boxes*, respectively, and correspond spatially with the images in **B** to **D**. (**B-1–D-1**) High-magnification images of AQP5 immunolabeling (*green*) in the cortical fiber cell regions shown in **A**. AQP5-containing cytoplasmic vesicles were primarily linear in morphology in the incipient fiber cells of the lens modiolus (*open arrowheads*) and spheroidal, linear in the cells outside of the lens modiolus (*closed arrowheads*). AQP5-containing cytoplasmic vesicles became slightly irregular in the outer cortex–inner cortex transitional region. (**B-2–D-2**) Replicate images of **B-1** to **D-1** depicting AQP5 immunolabeling and DAPI labeling only. (**B-3–D-3**) Enlarged images of AQP5-containing cytoplasmic vesicles are indicated by the *arrowheads* in **B-1** to **D-1**. The spheroidal and linear domains within AQP5-containing cytoplasmic vesicles vary in size up to a maximum width and length of approximately 3 µm and 20 µm, respectively. (**B-4–D-4**) Replicate images of **B-3** to **D-3** depicting AQP5 immunolabeling and DAPI labeling only. *Scale bars*: 100 µm (**A**), 10 µm (**B-1**, **B-2**, **C-1**, **C-2**, **D-1**, **D-2**), and 5 µm (**B-3**, **B-4**, **C-3**, **C-4**, **D-3**, **D-4**).

COX IV expression was similar to that of TOMM20, but we observed minimal calnexin expression in AQP5-containing cytoplasmic vesicles.

Despite AQP5 plasma membrane insertion in the bovine lens cortex, mitochondrial degradation occurs universally within the vertebrate ocular lens[32,35–38] and occurs through mitophagy in the mouse lens as BNIP3L/NIX expression, a mitophagy protein, is required for mitochondrial elimination to create the organelle-free zone.[39] In the chick lens, autophagosomes are TOMM20 positive and LC3B positive.[35] Thus, we hypothesized that AQP5- and TOMM20-containing cytoplasmic vesicles in bovine lens fiber cells might become

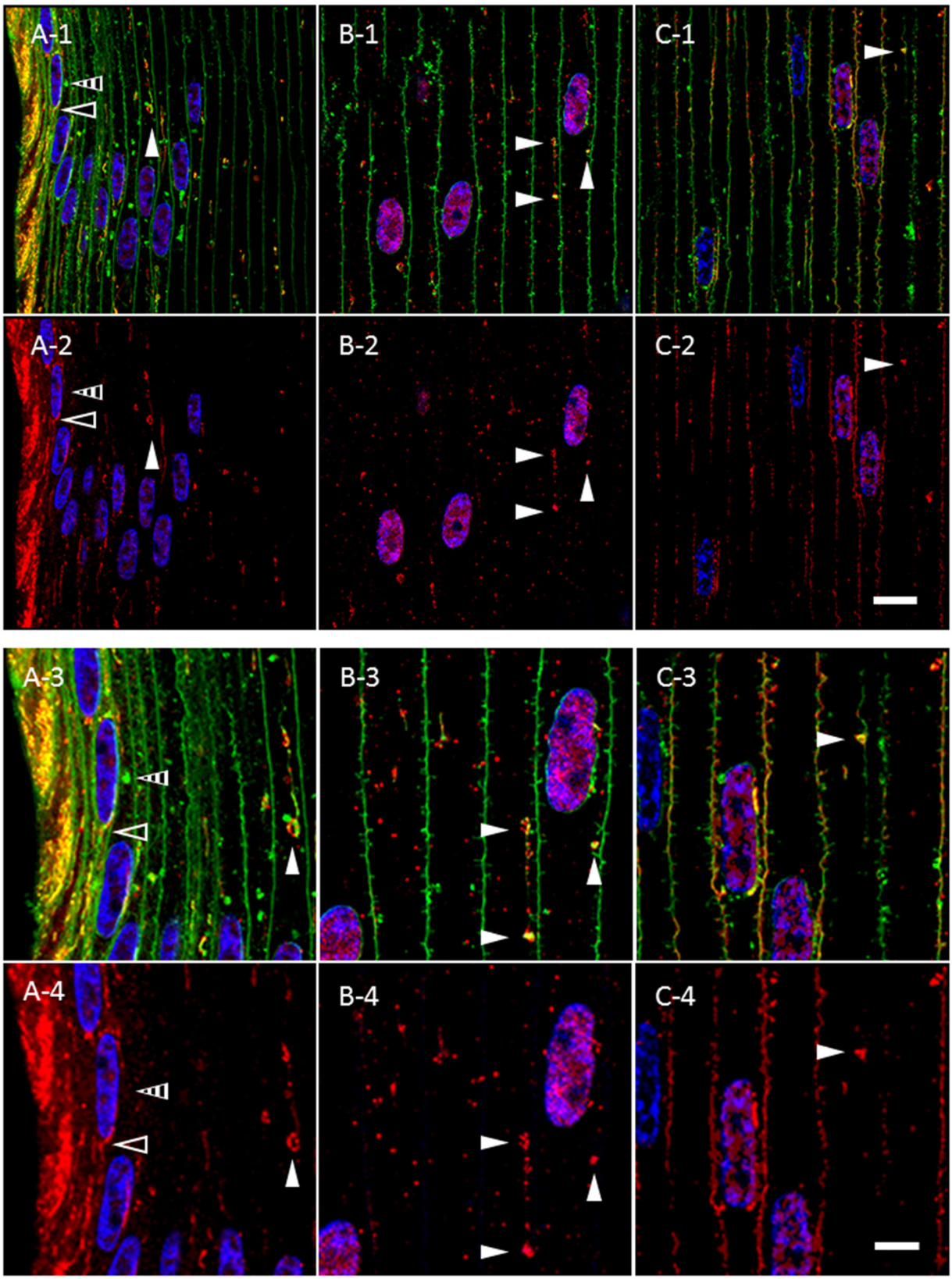

Figure 4. AQP5-containing, cytoplasmic vesicles represent a morphologically, distinct cluster of cytoplasmic vesicles in bovine lens cortical fiber cells outside the lens modiolus. (**A-1**–**C-1**) High-magnification confocal images of AQP5 immunolabeling (*red*) and DiI fluorescent labeling (*green*) in the peripheral outer cortex (**A-1**), medial outer cortex (**B-1**), and outer cortex–inner cortex transitional region (**C-1**) of the bovine lens as indicated in Figure 3A. In the lens modiolus (**A**), linear DiI-labeled cytoplasmic compartments (*open arrowheads*) overlap with linear, AQP5-containing cytoplasmic vesicles. In these cells, both AQP5-negative (*striped arrowheads*) and AQP5-containing (*closed white arrowheads*) DiI-labeled cytoplasmic structures are readily observable. In the peripheral outer cortical fiber cells outside of the lens modiolus,

Investigative Ophthalmology & Visual Science

medial outer cortex (**B**), and outer cortex–inner cortex transitional region (**C**), the spheroidal, linear DiI-labeled cytoplasmic compartments (*closed white arrowheads*) overlap with AQP5-containing, cytoplasmic vesicles with rare exceptions. (**A-2–C-2**) Replicate images of **A-1** to **C-1** with only AQP5 immunolabeling and DAPI labeling are displayed. (**A-3–C-3**) Enlarged images of DiI-labeled cytoplasmic structures are indicated by *arrowheads* in **A-1**, **B-1**, and **C-1**. Red puncta that do not colocalize with DiI represent nonspecific immunofluorescence based on normal IgG immunolabeling negative controls. (**A-4–C-4**) Replicate images of **A-3**, **B-3**, and **C-3** with only AQP5 immunolabeling and DAPI labeling displayed. *Scale bars*: 10 µm (**A-1**, **A-2**, **B-1**, **B-2**, **C-1**, **C-2**) and 5 µm (**A-3**, **A-4**, **B-3**, **B-4**, **C-3**, **C-4**).

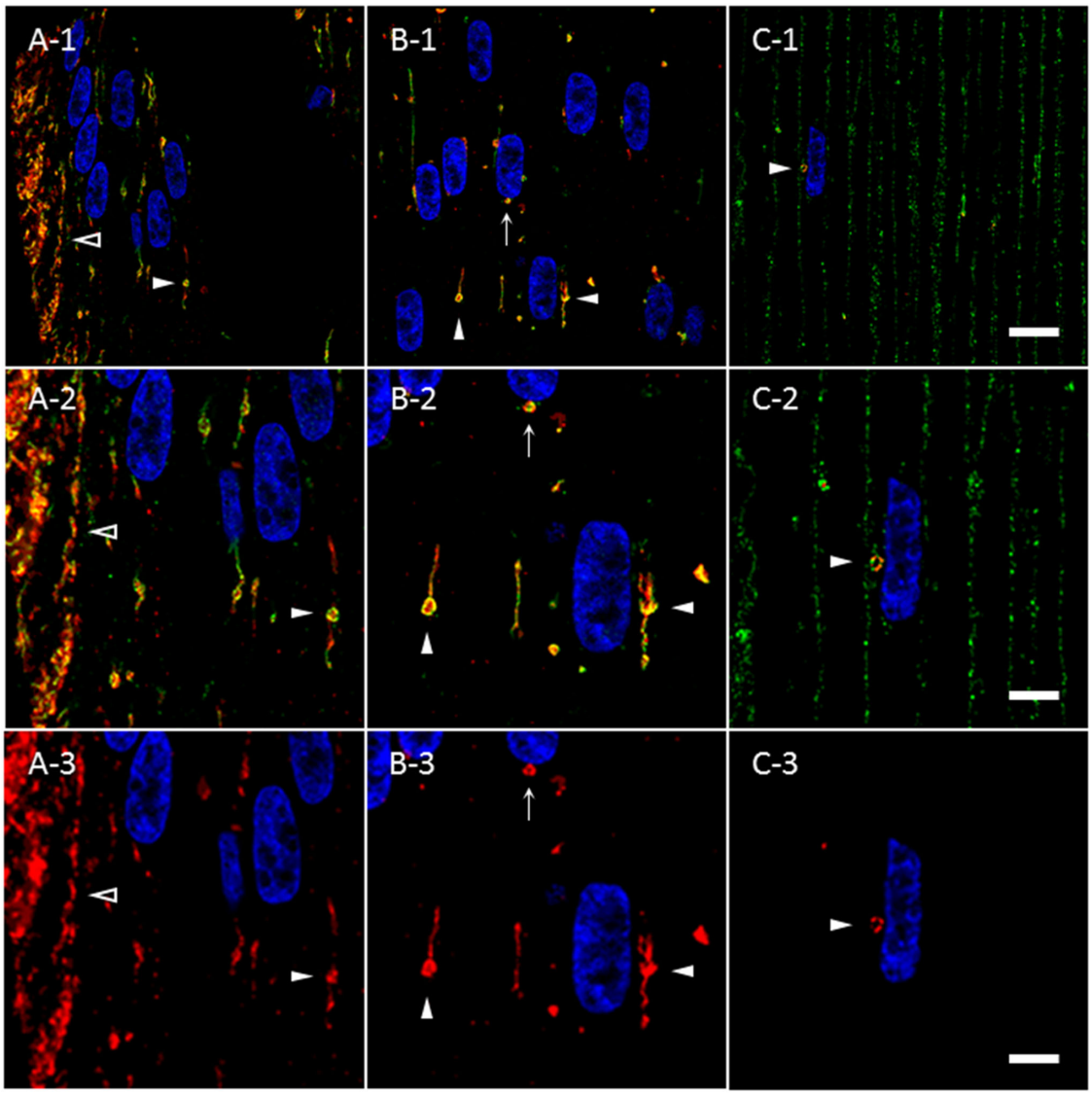

Figure 5. TOMM20 and AQP5 are co-expressed molecular markers for the same cluster of cytoplasmic vesicles in the bovine lens cortex. (**A-1–C-1**) High-magnification confocal images of AQP5 immunolabeling (*green*) and TOMM20 immunolabeling (*red*) in the peripheral outer cortex (**A**), medial outer cortex (**B**), and outer cortex–inner cortex transitional region (**C**) of the bovine lens as shown in Figure 3A. Linear (**A**, *open arrowheads*) and spheroidal, linear (**B**, **C**, *closed arrowheads*) AQP5-containing cytoplasmic vesicles and TOMM20-containing cytoplasmic vesicles colocalize in the outer cortex of bovine lenses. TOMM20-containing and AQP5-containing cytoplasmic vesicles are frequently apposed to fiber cell nuclei (**B**, *arrow*; **C**, *closed arrowhead*). (**A-2–C-2**) Enlarged images of AQP5-containing cytoplasmic vesicles indicated by *arrowheads* in **A-1**, **B-1**, and **C-1**. (**A-3–C-3**) Replicate images of **A-2**, **B-2**, and **C-2** with only TOMM20 immunolabeling and DAPI labeling displayed. *Scale bars*: 10 µm (**A-1**, **B-1**, **C-1**) and 5 µm (**A-2**, **A-3**, **B-2**, **B-3**, **C-2**, **C-3**).

autophagic vesicles and also express LC3B, an autophagy-specific molecular marker and peripheral membrane protein within autophagosomes, amphisomes, and autolysosomes. We analyzed TOMM20-containing cytoplasmic vesicles in the bovine lens for LC3B expression in bovine lens fiber cells (Fig. 6). In the lens modiolus, linear TOMM20-containing cytoplasmic vesicles are readily observable as in Figure 5 (Fig. 6A, open arrowheads), but LC3B expression in these structures is virtually undetectable. In peripheral outer cortical fiber cells outside of the lens modiolus, LC3B

Investigative Ophthalmology & Visual Science

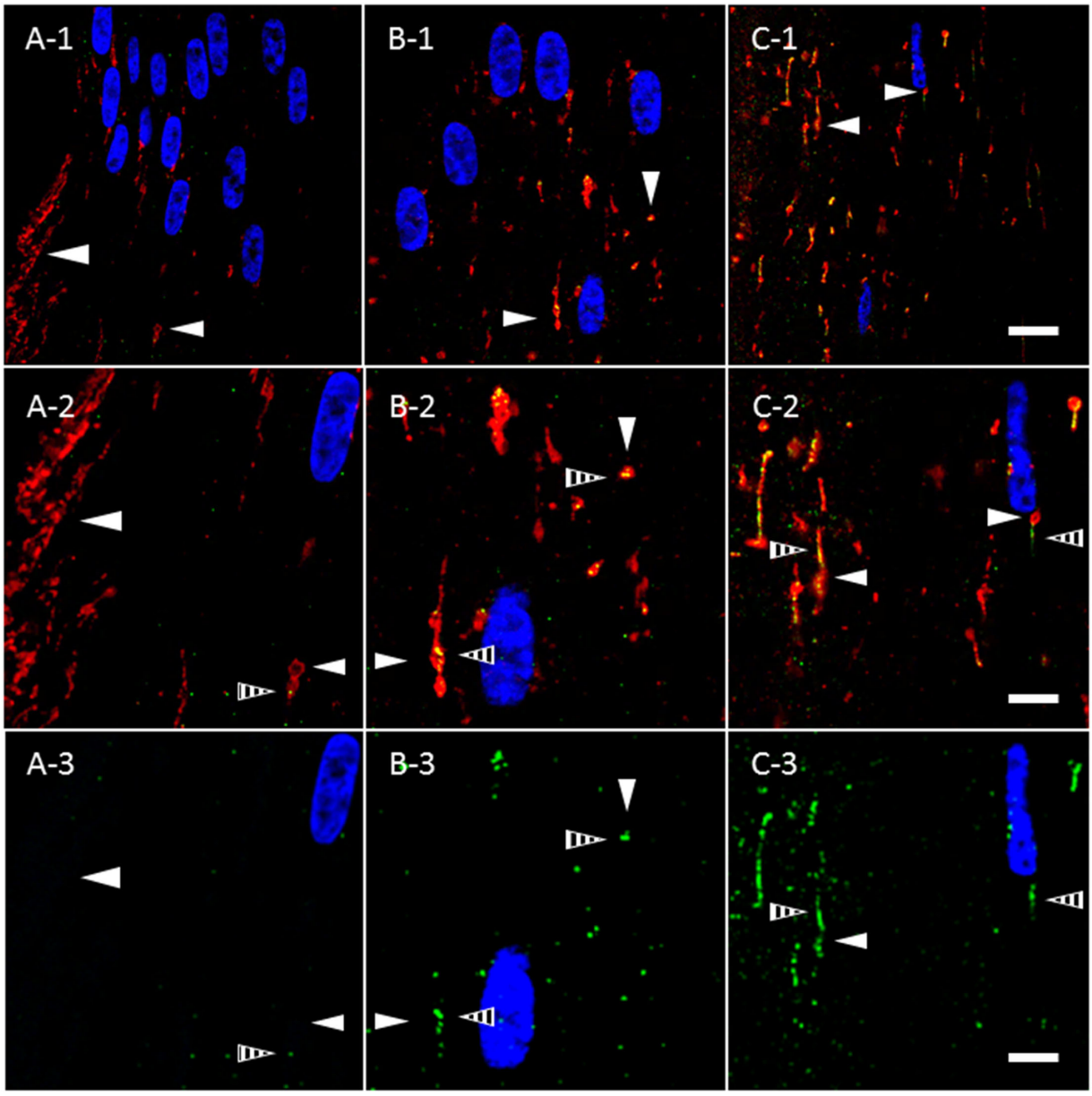

Figure 6. TOMM20-containing cytoplasmic vesicles express LC3B prior to complete AQP5 plasma membrane insertion in bovine lens cortical fiber cells. (**A-1–C-1**) High-magnification confocal images of TOMM20 immunolabeling (*red*) and LC3B immunolabeling (*green*) in the peripheral outer cortex (**A**), medial outer cortex (**B**), and outer cortex–inner cortex transitional region (**C**) of the bovine lens (Fig. 3A). In the peripheral outer cortex, LC3B is faintly expressed (**A**) in punctate, cytoplasmic vesicles (**A–C**, *striped arrowheads*). TOMM20-containing cytoplasmic vesicles (*closed arrowheads*) in the peripheral outer cortex colocalize minimally with LC3B. As outer cortical fiber cells mature, LC3B expression is upregulated; thus, LC3B-containing cytoplasmic vesicles are significantly larger and more abundant in the medial outer cortex (**B**) and outer cortex–inner cortex transitional region (**C**) relative to the peripheral outer cortex. LC3B colocalizes with the TOMM20-containing cytoplasmic vesicles in the medial outer cortex and the outer cortex–inner cortex transitional region (**B**, **C**). (**A-2–C-2**) Enlarged images of the TOMM20-containing cytoplasmic vesicles indicated by the *arrowheads* in **A-1**, **B-1**, and **C-1**. (**A-3–C-3**) Replicate images of **A-2**, **B-2**, and **C-2** with only LC3B immunolabeling and DAPI labeling displayed. *Scale bars*: 10 µm (**A-1**, **B-1**, **C-1**) and 5 µm (**A-2**, **A-3**, **B-2**, **B-3**, **C-2**, **C-3**).

expression (Fig. 6A, striped arrowheads) is sparse and sporadically localized to spheroidal, linear TOMM20-containing cytoplasmic vesicles (Fig. 6A, closed arrowheads). LC3B expression and colocalization within TOMM20-containing cytoplasmic vesicles increase as a function of fiber cell differentiation, suggesting that mitochondria, and thereby AQP5-containing cytoplasmic vesicles, are incorporated into autophagosomes and potentially into amphisomes and autolysosomes, as well. By the outer cortex–inner cortex transitional region, TOMM20-containing cytoplasmic vesicles appear to ubiquitously express LC3B (Figs. 6B, 6C). The morphology of LC3B-positive structures in the bovine lens outer cortex is interesting to note, as autophagosomes are typically globular or spherical rather than linear. There are special cases of autophagosomes with distinct morphology in the literature,[40,41] but the association

Investigative Ophthalmology & Visual Science

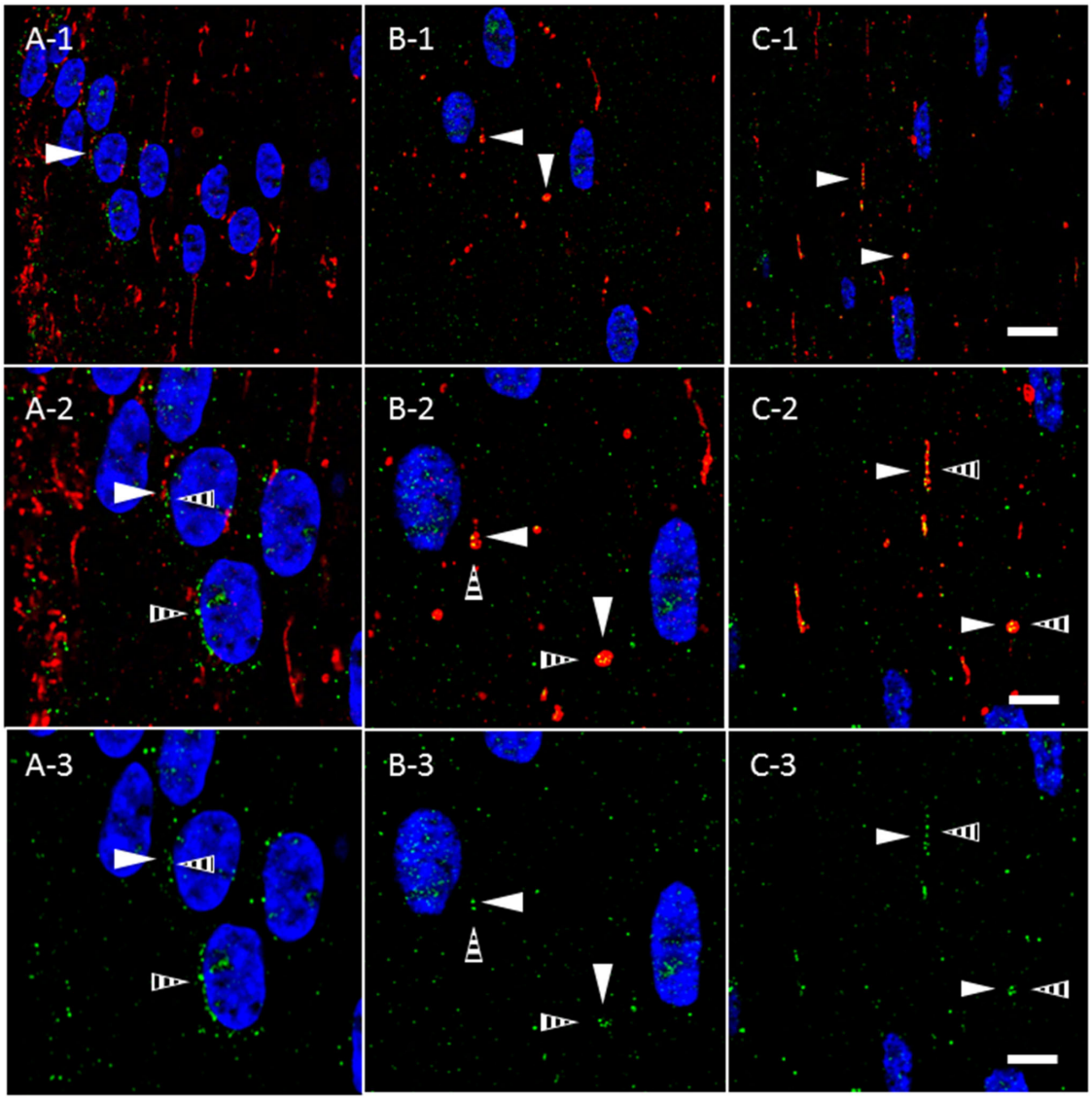

Figure 7. TOMM20-containing cytoplasmic vesicles express LIMP-2 prior to full AQP5 plasma membrane insertion in bovine lens cortical fiber cells. (**A-1–C-1**) High-magnification confocal images of TOMM20 immunolabeling (*red*) and LIMP-2 immunolabeling (*green*) in the peripheral outer cortex (**A**), medial outer cortex (**B**), and outer cortex–inner cortex transitional region (**C**) of the bovine lens (Fig. 3A). In the peripheral outer cortex, LIMP-2 is faintly expressed (**A**) in cytoplasmic vesicles (**A–C**, *striped arrowheads*). TOMM20-containing cytoplasmic vesicles (*closed arrowheads*) in the peripheral outer cortex partially colocalize with LIMP-2. LIMP-2 expression is upregulated with fiber cell differentiation and simultaneously increased in TOMM20-containing cytoplasmic vesicles. LIMP-2 colocalizes with the TOMM20-containing cytoplasmic vesicles in the medial outer cortex and the outer cortex–inner cortex transitional region (**B** and **C**). (**A-2–C-2**) Enlarged images of the TOMM20-containing cytoplasmic vesicles indicated by the *arrowheads* in **A-1**, **B-1**, and **C-1**. (**A-3–C-3**) Replicate images of **A-2**, **B-2**, and **C-2** with only LIMP-2 immunolabeling and DAPI labeling displayed. *Scale bars*: 10 µm (**A-1**, **B-1**, **C-1**) and 5 µm (**A-2**, **A-3**, **B-2**, **B-3**, **C-2**, **C-3**).

of LC3B with cytoplasmic structures that appear linear is atypical and will require additional study to clarify.

Autolysosomes containing mitochondria and in the process of mitophagy have been previously reported in the lens.[35,37,38] Given our observation of LC3B expression in AQP5- and TOMM20-containing cytoplasmic vesicles in bovine lens fiber cells, we hypothesized that a portion of these vesicles would also express specific autolysosomal and lysosomal molecular markers such as LIMP-2. We analyzed TOMM20-containing cytoplasmic vesicles in bovine cortical lens fiber cells for LIMP-2 expression (Fig. 7). In the lens modiolus, LIMP-2 expression in TOMM20-containing cytoplasmic vesicles is similar to that observed for LC3B. In peripheral outer cortical fiber cells outside of the lens modiolus, LIMP-2 expression (Fig. 7, striped arrows) is also sparse and rarely overlaps TOMM20-containing cytoplasmic vesicles (Fig. 7A, closed arrowheads). LIMP-2 expression in TOMM20-containing cytoplasmic vesicles also increases as a function of fiber cell differentiation. By the outer cortex–inner cortex transitional region, TOMM20-containing cytoplasmic vesicles express LIMP-2 with near ubiquity (Figs. 7B, 7C). LIMP-2 expression in the lens was confirmed via tandem mass spectrometry (Supplementary Fig. S3). These findings suggest that LC3B-positive autophagosomes

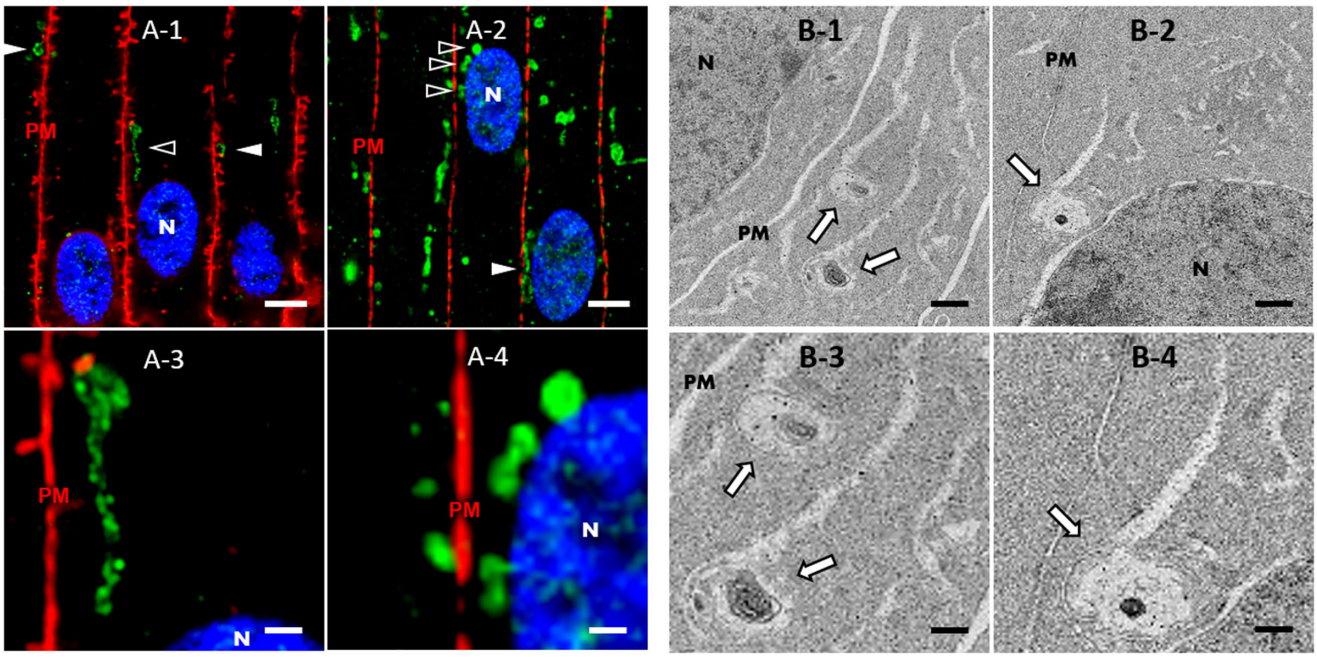

Figure 8. AQP5-containing cytoplasmic vesicles are congruent in subcellular localization with vesicular assemblies identified via TEM analysis in bovine lens cortical fiber cells. (**A**) High-resolution, confocal images of AQP5 immunofluorescence (*green*) in the medial outer cortex of the bovine lens. Plasma membranes (PM) are labeled with WGA (*red*) (**A-1**) or connexin 50 (*red*) (**A-2**). Cellular nuclei (N) are labeled with DAPI staining (*blue*). AQP5-containing cytoplasmic vesicles (*arrowheads*) are distinctive among fiber cell cytoplasmic vesicles in the bovine lens outer cortex (Fig. 4). AQP5-containing cytoplasmic vesicles are frequently in close proximity or apposed to fiber cell plasma membranes (**A-1**) and cellular nuclei (**A-2**). The structures indicated by *open arrowheads* in **A-1** and **A-2** are enlarged and shown in **A-3** and **A-4**, respectively. *Scale bars*: 5 µm (**A-1**, **A-2**) and 1 µm (**A-3**, **A-4**). (**B**) TEM images depicting vesicular assemblies of interest (*arrows*) in outer cortical fiber cells of the bovine lens in close proximity or apposed to the plasma membrane (**B-1**, **B-3**) or the nucleus (**B-2**, **B-4**). The structures indicated with arrows in **B-1** and **B-2** are enlarged and shown in **B-3** and **B-4**, respectively. *Scale bars*: 500 nm (**B-1**, **B-2**) and 250 nm (**B-3**, **B-4**).

merge with LIMP-2-positive lysosomes, possibly via an amphisome intermediate, to become autolysosomes after incorporation of AQP5-containing cytoplasmic vesicles.

Given these results, we hypothesized that TEM of bovine lens cortical fiber cells would reveal vesicular structures with similar morphology and subcellular localization to AQP5-containing cytoplasmic vesicles. Immunofluorescence analysis of bovine lens cryosections revealed that spheroidal AQP5-containing cytoplasmic vesicles are often in close proximity or apposed to cortical fiber cell plasma membranes (Fig. 8A-1, arrowheads) in the bovine lens. TEM analysis revealed vesicular assemblies in close proximity and apposed to (Figs. 8B-1–8B-4, arrows) bovine cortical fiber cell plasma membranes (Fig. 8, indicated by PM). Some of these vesicular assemblies present as spheroidal and some present as spheroidal with linear components attached. The vesicular assemblies of interest in our TEM images often contain multiple complex membranes. However, the resolution of vesicular assemblies in our TEM images requires improvement to unequivocally identify autophagic vesicles. We hypothesize that the vesicular assemblies detected in our TEM analysis are synonymous with AQP5-containing cytoplasmic vesicles detected in our immunofluorescence analysis based on subcellular localization and morphology.

AQP5 Vesicle-Plasma Membrane Localization

Further analysis of TEM images in the outer cortex showed vesicular assemblies with multiple complex membranes in very close proximity to the plasma membrane (Fig. 9). We regularly observed AQP5-containing cytoplasmic vesicles that appear to be docked with the plasma membrane in the medial outer cortex prior to AQP5 plasma membrane insertion (Figs. 9A-1–9A-3, arrowheads). In the outer cortex–inner cortex transitional region, similar AQP5-containing cytoplasmic vesicles appear to be docked to the plasma membrane (Figs. 9A-4–9A-6, arrowheads) where AQP5 insertion occurs. AQP5 signal occurs in the plasma membrane between strong Cx50 signals with some colocalization observed (Figs. 9A-5, 9A-6, arrows). In turn, we observed vesicular assemblies in close contact with the plasma membrane in bovine lens cortical fiber cells from the same regions (Fig. 9B-1, striped arrow). Although the overlap of AQP5 and Cx50 immunofluorescence and the close proximity of vesicular assemblies to the plasma membrane in our TEM data do not unequivocally demonstrate vesicular docking and fusion, these data are consistent with the hypothesis of unconventional protein secretion of AQP5 in the bovine lens cortex. Higher resolution studies are required to conclusively show docking and fusion processes.

Together, these data are consistent with the hypothesis of AQP5 plasma membrane insertion through unconventional protein secretion[42,43] in bovine lens cortical fiber cells via protein targeting to autophagosomes, to amphisomes, or to lysosomes prior to fusion with the plasma membrane. These processes, autophagosome secretion,[44–46] amphisome secretion,[47,48] and lysosome secretion,[47,49,50] respectively, are discrete mechanisms of secretion with unique molecular machineries. Secretory autophagosomes, but not degradative autophagosomes, specifically express

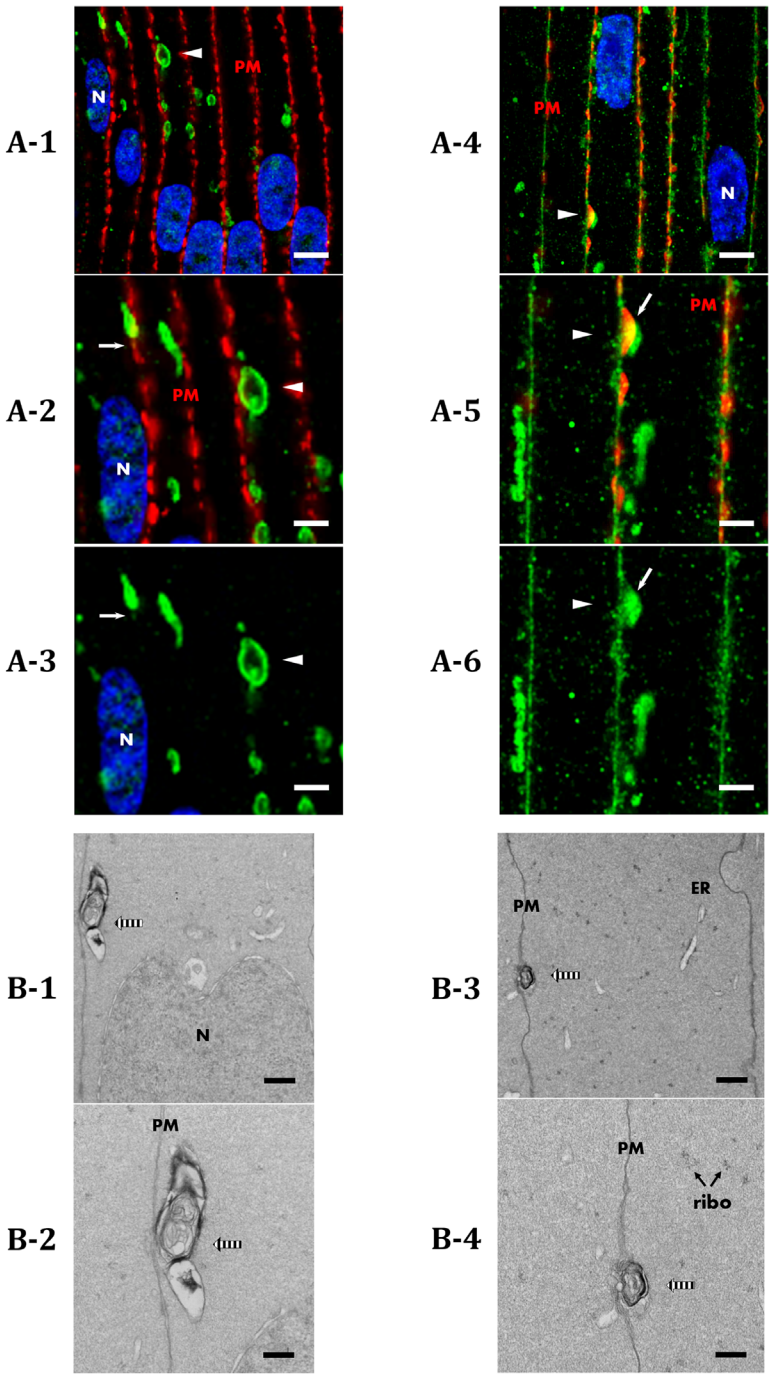

Figure 9. AQP5-containing cytoplasmic vesicles and vesicular assemblies identified via TEM analysis exhibit potential docking behavior in bovine lens cortical fiber cells. (**A**) High-resolution, confocal images of AQP5 immunofluorescence (*green*) in the medial outer cortex (**A-1**–**A-3**) and outer cortex–inner cortex transitional region (**A-4**–**A-6**) of the bovine lens. Plasma membranes (PM) are labeled with connexin 50. Cellular nuclei (N) are labeled with DAPI staining (*blue*). AQP5-containing cytoplasmic vesicles (*arrowheads*) appear in close apposition to and exhibit potential docking with fiber cell plasma membranes in the medial outer cortex (**A-1**). Docking of AQP5-containing cytoplasmic vesicles in the outer cortex–inner cortex transitional region (**A-4**) is expected to result in vesicular fusion, as full AQP5 plasma membrane insertion occurs prior to the inner cortex (Fig. 2). AQP5-containing cytoplasmic vesicles indicated with *arrowheads* in **A-1** and **A-4** are enlarged and shown in **A-2** and **A-3** and in **A-5** and **A-6**, respectively. AQP5 plasma membrane insertion is denoted by the *arrows* in **A-2**, **A-3**, **A-5**, and **A-6**. *Scale bars*: 5 µm (**A-1**, **A-4**) and 2.5 µm (**A-2**, **A-3**, **A-5**, **A-6**). (**B**) TEM images of vesicular assemblies of interest (*striped arrows*) in the bovine lens outer cortex exhibit potential docking (**B-1**–**B-4**) to the fiber cell plasma membrane. The vesicular assemblies in **B-1** and **B-3** are enlarged and shown in **B-2** and **B-4**, respectively. These structures are congruent with AQP5-containing cytoplasmic vesicle in subcellular localization. The endoplasmic reticulum (ER) and ribosomes (ribo) are also visible. *Scale bars*: 500 nm (**B-1**, **B-3**) and 250 nm (**B-2**, **B-4**).

Investigative Ophthalmology & Visual Science

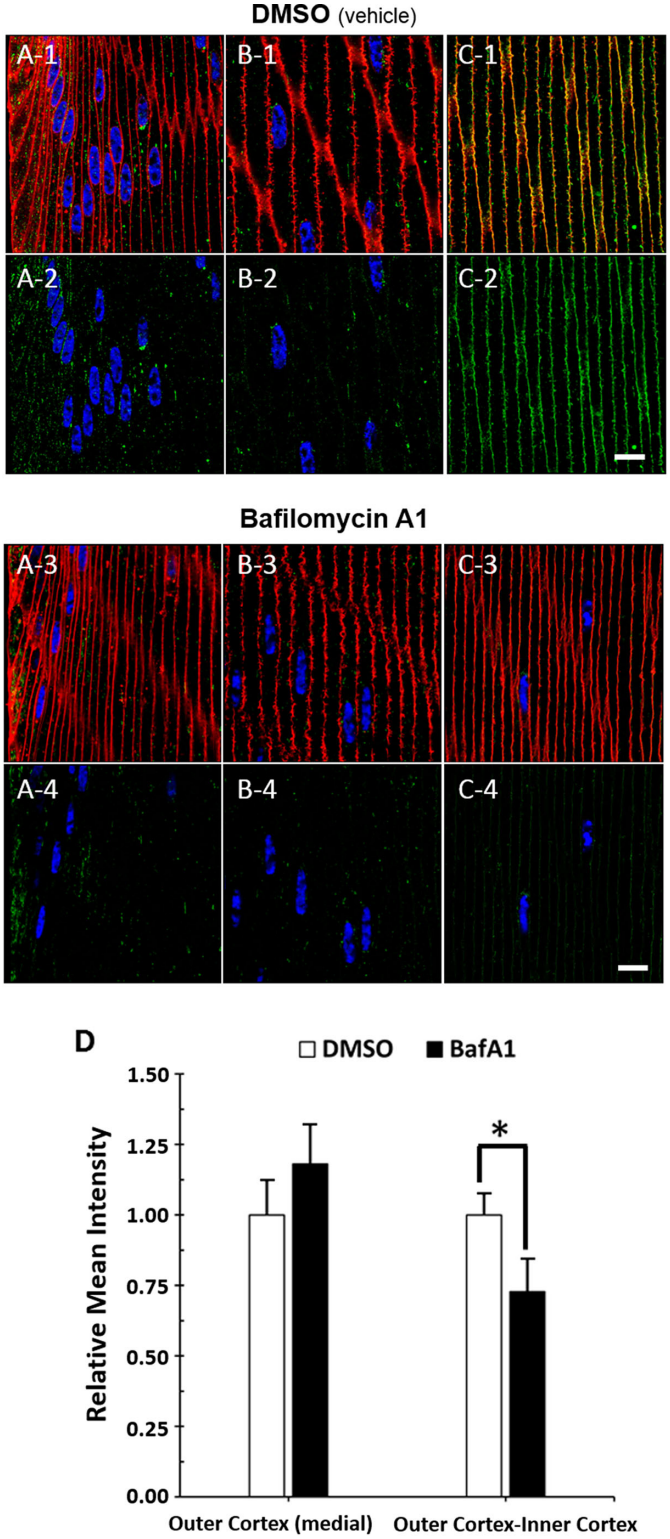

Figure 10. Autophagosome–lysosome fusion inhibition via bafilomycin A1 treatment decreases AQP5 plasma membrane expression in the bovine lens cortex. (**A-1–C-1**) High-magnification confocal images of AQP5 immunolabeling (*green*) and WGA labeling (*red*) in the peripheral outer cortex (**A**), medial outer cortex (**B**), and outer cortex–inner cortex transitional region (**C**) of the bovine lens following 24-hour ex vivo culture in complete M199 medium with vehicle (0.1% DMSO) (Fig. 3A). (**A-2–C-2**) Replicate images of **A-1**, **B-1**, and **C-1** with only AQP5 immunolabeling and DAPI labeling displayed. (**A-3–C-3**) High-magnification confocal images of AQP5 immunolabeling (*green*) and WGA labeling (*red*) in the peripheral outer cortex (**A**), medial outer cortex (**B**), and outer cortex–inner cortex transitional region (**C**) of the bovine lens following 24-hour ex vivo culture with 10-nM bafilomycin A1 (Fig. 3A). (**A-4–C-4**) Replicate images of **A-3**, **B-3**, and **C-3** with only AQP5 immunolabeling and DAPI labeling displayed. *Scale bars*: 10 µm (**A–C**). (**D**) Quantification and statistical analysis of the relative AQP5 plasma membrane expression, defined as relative mean intensity, in fiber cells of the medial outer cortex and outer cortex–inner cortex transitional region of bovine lens cryosections following 24-hour ex vivo culture with vehicle control 0.1% DMSO ($n = 7$) or with 10-nM bafilomycin A1 (BafA1, $n = 8$). Two-tailed Student's *t*-test was significant (*) at $P = 0.032$.

Investigative Ophthalmology & Visual Science

the SNARE protein vesicle-trafficking protein Sec22β.[47,51] We found that TOMM20-containing mitochondria, the signals of which overlap almost entirely with AQP5-containing cytoplasmic vesicles (Fig. 5), lacked apparent Sec22β expression (Supplementary Fig. S4).

The absence of Sec22β co-labeling with TOMM20-containing mitochondria analyses suggests that AQP5-containing cytoplasmic vesicles become LC3B-containing autophagosomes or amphisomes that fuse with lysosomes that then undergo lysosome secretion in the outer cortex–inner cortex transitional region. To test this hypothesis, we examined AQP5 plasma membrane expression in ex vivo cultured bovine lenses treated with 10-nM bafilomycin A1 for 24 hours to inhibit autophagosome–lysosome fusion and thereby reduce lysosome secretion (Fig. 10). Following ex vivo lens culture, AQP5 expression can still be detected in the bovine lens cortex (Figs. 10A–10C). Relative AQP5 expression (i.e., mean fluorescence intensity of AQP5 with bafilomycin A1 treatment relative to vehicle control) was quantified in fiber cell plasma membranes in the bovine lens medial outer cortex and outer cortex-inner cortex transitional region (Fig. 10D). Confocal microscopy imaging parameters used to acquire ex vivo cultured bovine lens data were kept consistent for quantitative comparison. Despite sample variation, there was no significant difference in relative AQP5 expression in fiber cell plasma membranes of the medial outer cortex. In contrast, relative AQP5 fiber cell plasma membrane expression in the outer cortex–inner cortex transitional region, where full insertion of AQP5-containing cytoplasmic vesicles with fiber cell plasma membrane occurs, was decreased by approximately 27%. These results are consistent with our hypothesis of AQP5 lysosome secretion in the bovine lens.

Discussion

The goals of this study were to determine how bovine lenticular AQP5 expression patterns compare to other mammalian lenses, to determine the subcellular localization of AQP5-containing cytoplasmic vesicles, and to identify potential trafficking mechanisms of AQP5-containing cytoplasmic vesicles to the plasma membrane. In this study, we revealed that bovine lens AQP5 expression patterns are similar to that of other mammalian lenses, being cytoplasmic in lens epithelial cells and young, differentiating lens fiber and then shifting to lens fiber cell plasma membranes with cellular maturation. We have also for the first time defined AQP5 subcellular localization in ocular lens cortical fiber cells in detail and discovered evidence of cytoplasmic AQP5 trafficking to the plasma membrane in these cells via lysosome secretion, a novel mechanism of aquaporin trafficking.

AQP5 spatial expression has previously been investigated in mouse,[12,15–17] rat,[12,17] rabbit,[8] and human[12] lenses. Although Grey et al.[12] validated AQP5 expression in bovine lenses via western blot analysis, this study represents the first histological study of AQP5 spatial expression in the bovine lens. AQP5 is expressed throughout the bovine lens, being cytoplasmic in epithelial and fiber cells and gradually trafficking to plasma membrane during fiber cell differentiation (Fig. 1). This spatial expression pattern is consistent with previously studied lenses and further suggests that this general expression pattern is characteristic of AQP5 expression in all mammalian lenses. In bovine lenses, we measured AQP5 plasma membrane insertion to occur at a normalized r/a value of 0.958 (Fig. 2). Grey et al.[12] defined this value in mouse and rat lenses as $r/a = 0.95$ and $r/a = \sim 0.75$ to ~ 0.65, respectively.[12] This equivalence suggests similarity in regulation of AQP5 plasma membrane insertion in mouse and bovine lenses relative to rat lenses, but the implications of these values remain to be investigated. AQP5 expression in differentiating bovine outer cortical fiber cell nuclei becomes apparent as fiber cells exit the lens modiolus (Figs. 1C, 1D) and disappears as AQP5 trafficks to the plasma membrane (Figs. 1E, 1F). Cho et al.[52] demonstrated that AQP5 trafficks to the nucleus in rat parotid gland cells following treatment with the muscarinic acetylcholine receptor agonist cevimeline, resulting in reduction in the size of cellular nuclei and a change in the morphology of cellular nuclei from smooth and circular to rough and irregular. We speculate that nuclear localization of AQP5 in the bovine lens outer cortex may play a role in the shrinkage of fiber cell nuclei and change in their morphology from smooth to irregular during cellular differentiation as occurs in the inner cortex (Figs. 1E, 1F). We seek to test this hypothesis in future studies.

To the best of our knowledge, this is also the first study to characterize AQP5-containing cytoplasmic vesicles in a mammalian lens for intrinsic properties such as morphology or molecular composition. The presence of micrometer-scale linear and spheroidal, linear AQP5-containing cytoplasmic compartments (Fig. 3) is a novel finding in cortical lens fiber cells. Within bovine cortical lens fiber cells, AQP5-containing cytoplasmic vesicles are also morphologically distinct (Figs. 4A-3, 4A-4) which enables their identification via downstream TEM analysis.

Molecular analysis revealed that AQP5-containing cytoplasmic vesicles and mitochondria appear to be nearly indistinguishable cytoplasmic compartments in bovine lens cortical fiber cells. TOMM20 (Fig. 5), a protein subunit within the translocase of the outer mitochondrial membrane, and COX IV (Supplementary Fig. S1), a mitochondrial marker protein in the electron transport chain, both colocalize to AQP5-containing cytoplasmic vesicles in bovine lens cortical fiber cells, suggesting that AQP5 is incorporated into either mitochondria or mitochondria-containing cytoplasmic vesicles. Calnexin immunofluorescence analysis suggested that AQP5-containing cytoplasmic vesicles are not endoplasmic reticular compartments (Supplementary Fig. S2).

Mitochondria undergo autophagic degradation to generate an organelle-free zone (OFZ) in the lens to prevent light scatter.[35] TOMM20 colocalizes with LC3B, a specific protein marker of autophagosomes and amphisomes, in the embryonic chick lens prior to mitochondrial degradation. Immunofluorescence analysis revealed LC3B colocalization with TOMM20 in bovine lens cortical fiber cells (Fig. 6) that peaked within the outer cortex–inner cortex transitional region. LIMP-2 is a β-glucocerebrosidase receptor and specific protein marker of lysosomes,[53] and the colocalization of LIMP-2 with TOMM20 (Fig. 7), similar to LC3B, suggests lysosomal involvement in mitochondrial degradation. This finding is in agreement with previous data showing that LC3B expression peaks and autolysosomes are abundant in the outer cortex–inner cortex transitional region in mice just prior to mitochondrial elimination to form the OFZ.[37,38,54] TOMM20 and LC3B immunolabeling fade to become undetectable in mature fiber cells. AQP5 also is fully inserted into bovine lens fiber cell plasma membranes in

Investigative Ophthalmology & Visual Science

the outer cortex–inner cortex transitional region. The disappearance of TOMM20 and LC3B immunolabeling is consistent with mitochondrial degradation via incorporation into autophagosomes that merge with lysosomes via an amphisome intermediate to become autolysosomes. This observation is also consistent with the conservation of mitochondrial autophagy in the lens across species and TEM analysis of fiber cells in human and embryonic chick lenses, as reported by Costello et al.,[35] in which mitochondria are incorporated into autolysosomes. Genetic deletion studies suggest that lenticular mitochondrial autophagy is specific and technically mitophagy in the mouse lens.[39] This possibility remains to be tested in the bovine lens. Nevertheless, our data are consistent with the hypothesis that AQP5 undergoes unconventional protein secretion via autolysosomes in a manner similar to the thrombopoietin receptor Mpl.[55] The amphisome intermediate required for autolysosome formation remains to be identified histologically, and direct amphisome secretion via this amphisome intermediate in a manner similar to glycophorin A[56] remains a potential additional mechanism of AQP5-containing cytoplasmic vesicle secretion.

The persistence of AQP5 immunolabeling despite apparent mitochondrial degradation and AQP5 plasma membrane insertion is consistent with the hypothesis that AQP5-containing cytoplasmic vesicles are trafficked to the plasma membrane through the unconventional protein secretion pathway of lysosome secretion.[49] TEM analysis in bovine lens cortical fiber cells revealed vesicular assemblies with complex membranes with similar subcellular localization to AQP5-containing cytoplasmic vesicles (Fig. 8). Furthermore, immunofluorescence and TEM analysis respectively showed that AQP5-containing cytoplasmic structures and vesicular assemblies with complex membranes exhibit potential docking behavior with fiber cell plasma membranes in the medial outer cortex–inner cortex transitional region where AQP5 plasma membrane insertion primarily occurs (Fig. 9). Although it is tempting to speculate on the identity of vesicular assemblies present in our TEM data, higher resolution electron microscopy is needed to unequivocally identify fusion processes and potential mitochondria and autophagic vesicles (i.e., autophagosomes, amphisomes, and autolysosomes) in our TEM data.

Nevertheless, to the best of our knowledge, this is the first study to report autolysosome secretion as potential trafficking mechanism of plasma membrane insertion for AQP5, for aquaporins as a protein family in any tissue, and for any protein in lens fiber cells. The absence of Sec22β colocalization with TOMM20 (Supplementary Fig. S4) suggests that mitochondria and therefore AQP5 are not incorporated into secretory autophagosomes and that AQP5-containing cytoplasmic vesicles undergo autolysosome secretion and potentially amphisome secretion, as well. Autophagosome secretion, amphisome secretion, and lysosome secretion are classified as Type III unconventional protein secretion mechanisms.[43,47] Thus, although putative mitochondrial degradation through autophagy in bovine lens cortical fiber cells is consistent with other mammalian lenses, our data support the hypothesis that AQP5 is trafficked in bovine lenses through secretory autolysosomes via LC3B-containing autophagosomes. Results from bafilomycin A1 treatment of ex vivo cultured bovine lenses also support this hypothesis (Fig. 10). Upon treatment, relative AQP5 fiber cell plasma membrane expression in bovine lenses decreased by approximately 27% in the outer cortex–inner cortex transitional region, where AQP5 plasma membrane insertion primarily occurs (Fig. 10D). This is consistent with bafilomycin A1 inhibition of autophagosome–lysosome fusion and an accumulation of AQP5-containing autophagosomes unable to mature into autolysosomes for secretion.

Results from bafilomycin A1 treatment also provide further evidence that AQP5 functions as a regulatory water channel whose trafficking is inducible in the mammalian lens. Petrova et al.[17,21] have previously demonstrated dynamic AQP5 subcellular localization changes in response to changes in zonular tension via mechanosensitive transient receptor potential vanilloid 1 (TRPV1) channel agonism. Because AQP5 plasma membrane insertion significantly increases fiber cell water permeability in both mouse and rat lenses,[17] regulation of AQP5 subcellular localization can alter lens water homeostasis. Whether regulation of AQP5 subcellular localization via TRPV1 channels involves lysosome secretion remains to be investigated.

In non-lenticular tissues, cytoplasmic AQP5 undergoes regulated secretion to the plasma membrane in the salivary glands and in model cell systems upon M_3 muscarinic acetylcholine receptor (AChR) activation,[57,58] β-adrenergic receptor activation,[15,59,60] TRPV4 activation,[61,62] and osmotic perturbation.[61,62] Downstream signal transduction effectors of these activators such as nitric oxide, protein kinase G, protein kinase A (PKA) activity, and calcium have all been implicated in the alteration of AQP5 plasma membrane trafficking. To our knowledge, this is the first study to characterize the subcellular localization of cytoplasmic AQP5 vesicles targeted to the plasma membrane for regulated secretion. Our results are consistent with a novel mechanism of cytoplasmic AQP5 trafficking to the plasma membrane. The effects of nonlenticular effector proteins, such as the β-adrenergic receptors, or corresponding downstream effectors such as PKA on AQP5 plasma membrane trafficking in the lens remain to be investigated.

In addition, our results demonstrate possible AQP5 expression in viable mitochondria, which, if confirmed, along with aquaporin-8 (AQP8)[63] and aquaporin-9 (AQP9),[64] would represent the third aquaporin discovered in mitochondria. These results raise a variety of questions about the conservation of this AQP5 unconventional protein secretion across mammalian lenses and the implications of AQP5 in active mitochondria. Mitochondrial AQP8 and AQP9 function as peroxiporins and thereby resist accumulation of the reactive oxygen species H_2O_2, a byproduct of aerobic respiration that is detrimental to proper mitochondrial function.[65–68] AQP8 is expressed in the lens epithelial cells and exhibits peroxiporin function in vitro in cultured human lens epithelial cells.[24,69] AQP5 also functions as a peroxiporin facilitating H_2O_2 transport in transfected cells[24,70] and in the lens, with wild-type mouse lenses containing significantly more H_2O_2 content relative to AQP5 knockout mouse lenses.[24] Of note is the reported crosstalk between autophagy and oxidative stress,[71] in which H_2O_2 blocks the progression of autophagy via reversibly inhibition of ATG4.[72] Thus, AQP5 peroxiporin function is a plausible role for AQP5 incorporation into mitochondria and autophagic vesicles in the bovine lens fiber cells, and it is reasonable to conjecture potential roles for AQP5 in regulating mitochondrial viability and autophagic induction in the bovine lens. Future studies should address these and other relevant exciting questions both in the mammalian lens and in other tissues expressing AQP5.

Investigative Ophthalmology & Visual Science

Conclusions

In summary, bovine lenticular AQP5 expression patterns are similar to AQP5 expression patterns in other mammalian lenses, as AQP5 is cytoplasmic in epithelial cells and young fiber cells and then gradually trafficks to the plasma membrane. In the bovine lens, trafficking presumably occurs via unconventional protein secretion during fiber cell differentiation. In outer cortical bovine lens fiber cells, cytoplasmically expressed AQP5 is first associated with TOMM20-positive mitochondria and thereafter localized to LC3B-positive autophagosomes that merge with lysosomes to become LIMP-2-positive autolysosomes. Based on the loss of TOMM20 and COX IV immunofluorescence and incorporation of AQP5 into the plasma membrane, these autolysosomes potentially degrade mitochondria in differentiating lens fiber cells and appear to undergo plasma membrane insertion through a process of autolysosome secretion and potentially amphisome secretion. AQP5 expression in the plasma membrane is bafilomycin A1 sensitive, suggesting the importance of autophagosome-lysosome fusion for AQP5 plasma membrane insertion in the bovine lens.

Acknowledgments

The authors thank Evan Krystofiak, of the Vanderbilt Cell Imaging Shared Resource electron microscopy core, for his role in the acquisition and interpretation of our transmission electron microscopy data.

Supported by grants from the National Institutes of Health (R01 EY013462 and P30 EY008126). Confocal imaging, electron microscopy sample preparation, and transmission electron microscopy were performed through the use of the Vanderbilt Cell Imaging Shared Resource, which is supported by grants from the National Institutes of Health (CA68485, DK20593, DK58404, DK59637, and EY08126). The ZEISS LSM880 confocal microscope was acquired through a National Institutes of Health equipment grant (S10 OD021630).

Disclosure: **R.B. Gletten**, None; **L.S. Cantrell**, None; **S. Bhattacharya**, None; **K.L. Schey**, None

References

1. Cramer A. *Het Accommodatievermogen Dere Oogen Physiologisch Toegelicht*. Haarlem, the Netherlands: De erven Loosjes; 1853.
2. Den Tonkelaar I, Henkes HE, Van Leersum GK. Antonie Cramer's explanation of accommodation. *Doc Ophthalmol*. 1990;74:87–93.
3. Petrash J. Aging and age-related diseases of the ocular lens and vitreous body. *Invest Ophthalmol Vis Sci*. 2013;54:ORSF54-9.
4. Shi Y, Barton K, De Maria A, Petrash JM, Shiels A, Bassnett S. The stratified syncytium of the vertebrate lens. *J Cell Sci*. 2009;122:1607–1615.
5. Broekhuyse RM, Kuhlmann ED, Stols ALH. Lens membranes II. Isolation and characterization of the main intrinsic polypeptide (MIP) of bovine lens fiber membranes. *Exp Eye Res*. 1976;23:365–371.
6. Bok D, Dockstader J, Horwitz J. Immunocytochemical localization of the lens main intrinsic polypeptide (MIP26) in communicating junctions. *J Cell Biol*. 1982;92:213–220.
7. Fitzgerald PG, Bok D, Horwitz J. Immunocytochemical localization of the main intrinsic polypeptide (MIP) in ultrathin frozen sections of rat lens. *J Cell Biol*. 1983;97:1491–1499.
8. Bogner B, Schroedl F, Trost A, et al. Aquaporin expression and localization in the rabbit eye. *Exp Eye Res*. 2016;147:20–30.
9. Hasegawa H, Lian SC, Finkbeiner WE, Verkman AS. Extrarenal tissue distribution of CHIP28 water channels by in situ hybridization and antibody staining. *Am J Physiol*. 1994;266:C893–C903.
10. Wang Z, Han J, Schey KL. Spatial differences in an integral membrane proteome detected in laser capture microdissected samples. *J Proteome Res*. 2008;7:2696–2702.
11. Bassnett S, Wilmarth PA, David LL. The membrane proteome of the mouse lens fiber cell. *Mol Vis*. 2009;15:2448–2463.
12. Grey AC, Walker KL, Petrova RS, et al. Verification and spatial localization of aquaporin-5 in the ocular lens. *Exp Eye Res*. 2013;108:94–102.
13. Agre P, Sasaki S, Chrispeels MJ. Aquaporins: a family of water channel proteins. *Am J Physiol*. 1993;265:F461.
14. Ruiz-Ederra J, Verkman AS. Accelerated cataract formation and reduced lens epithelial water permeability in aquaporin-1-deficient mice. *Invest Ophthalmol Vis Sci*. 2006;47:3960–3967.
15. Sindhu Kumari S, Varadaraj M, Yerramilli VS, Menon AG, Varadaraj K. Spatial expression of aquaporin 5 in mammalian cornea and lens, and regulation of its localization by phosphokinase A. *Mol Vis*. 2012;18:957–967.
16. Petrova RS, Schey KL, Donaldson PJ, Grey AC. Spatial distributions of AQP5 and AQP0 in embryonic and postnatal mouse lens development. *Exp Eye Res*. 2015;132:124–135.
17. Petrova RS, Webb KF, Vaghefi E, Walker K, Schey KL, Donaldson PJ. Dynamic functional contribution of the water channel AQP5 to the water permeability of peripheral lens fiber cells. *Am J Physiol*. 2018;314:C191–C201.
18. Wang Z, Han J, David LL, Schey KL. Proteomics and phosphoproteomics analysis of human lens fiber cell membranes. *Invest Ophthalmol Vis Sci*. 2013;54:1135–1143.
19. Barandika O, Ezquerra-Inchausti M, Anasagasti A, et al. Increased aquaporin 1 and 5 membrane expression in the lens epithelium of cataract patients. *Biochim Biophys Acta*. 2016;1862:2015–2021.
20. Tang S, Di G, Hu S, Liu Y, Dai Y, Chen P. AQP5 regulates vimentin expression via miR-124-3p.1 to protect lens transparency. *Exp Eye Res*. 2021;205:108485.
21. Petrova RS, Bavana N, Zhao R, Schey KL, Donaldson PJ. Changes to zonular tension alters the subcellular distribution of AQP5 in regions of influx and efflux of water in the rat lens. *Invest Ophthalmol Vis Sci*. 2020;61:36.
22. Karasawa K, Tanaka A, Jung K, et al. Patterns of aquaporin expression in the canine eye. *Vet J*. 2011;190:e72–e77.
23. Sindhu Kumari S, Varadaraj K. Aquaporin 5 knockout mouse lens develops hyperglycemic cataract. *Biochem Biophys Res Commun*. 2013;441:333–338.
24. Varadaraj K, Kumari SS. Lens aquaporins function as peroxiporins to facilitate membrane transport of hydrogen peroxide. *Biochem Biophys Res Commun*. 2020;524:1025–1029.
25. Hu S, Wang B, Qi Y, Lin H. The Arg233Lys AQP0 mutation disturbs aquaporin0-calmodulin interaction causing polymorphic congenital cataract. *PLoS One*. 2012;7:e37637.
26. Senthil Kumar G, Kyle JW, Minogue PJ, et al. An MIP/AQP0 mutation with impaired trafficking and function underlies an autosomal dominant congenital lamellar cataract. *Exp Eye Res*. 2013;110:136–141.
27. Kumari SS, Gandhi J, Mustehsan MH, Eren S, Varadaraj K. Functional characterization of an AQP0 missense mutation, R33C, that causes dominant congenital lens cataract, reveals impaired cell-to-cell adhesion. *Exp Eye Res*. 2013;116:371–385.

Investigative Ophthalmology & Visual Science

28. Song Z, Wang L, Liu Y, Xiao W. A novel nonsense mutation in the MIP gene linked to congenital posterior polar cataracts in a Chinese family. *PLoS One*. 2015;10:e0119296.
29. Shiels A, Bassnett S, Varadaraj K, et al. Optical dysfunction of the crystalline lens in aquaporin-0-deficient mice. *Physiol Genomics*. 2001;7:179–186.
30. Azlina A, Javkhlan P, Hiroshima Y, et al. Roles of lysosomal proteolytic systems in AQP5 degradation in the submandibular gland of rats following chorda tympani parasympathetic denervation. *Am J Physiol*. 2010;299:1106–1117.
31. Huang Y, Shi X, Mao Q, et al. Aquaporin 5 is degraded by autophagy in diabetic submandibular gland. *Sci China Life Sci*. 2018;61:1049–1059.
32. Basu S, Rajakaruna S, Reyes B, Van Bockstaele E, Menko AS. Suppression of MAPK/JNK-MTORC1 signaling leads to premature loss of organelles and nuclei by autophagy during terminal differentiation of lens fiber cells. *Autophagy*. 2014;10:1193–1211.
33. Mathias RT, Rae JL, Baldo GJ. Physiological properties of the normal lens. *Physiol Rev*. 1997;77:21–50.
34. Bassnett S, Beebe DC. Coincident loss of mitochondria and nuclei during lens fiber cell differentiation. *Dev Dyn*. 1992;194:85–93.
35. Costello MJ, Brennan LA, Basu S, et al. Autophagy and mitophagy participate in ocular lens organelle degradation. *Exp Eye Res*. 2013;116:141–150.
36. Morishita H, Mizushima N. Autophagy in the lens. *Exp Eye Res*. 2016;144:22–28.
37. Morishita H, Eguchi S, Kimura H, et al. Deletion of autophagy-related 5 (Atg5) and Pik3c3 genes in the lens causes cataract independent of programmed organelle degradation. *J Biol Chem*. 2013;288:11436–11447.
38. McWilliams TG, Prescott AR, Villarejo-Zori B, Ball G, Boya P, Ganley IG. A comparative map of macroautophagy and mitophagy in the vertebrate eye. *Autophagy*. 2019;15:1296–1308.
39. Brennan LA, McGreal-Estrada R, Logan CM, Cvekl A, Menko AS, Kantorow M. BNIP3L/NIX is required for elimination of mitochondria, endoplasmic reticulum and Golgi apparatus during eye lens organelle-free zone formation. *Exp Eye Res*. 2018;174:173–184.
40. Uemura T, Yamamoto M, Kametaka A, et al. A cluster of thin tubular structures mediates transformation of the endoplasmic reticulum to autophagic isolation membrane. *Mol Cell Biol*. 2014;34:1695–1706.
41. Zhuang X, Chung KP, Cui Y, et al. ATG9 regulates autophagosome progression from the endoplasmic reticulum in Arabidopsis. *Proc Natl Acad Sci USA*. 2017;114:E426–E435.
42. Rabouille C. Pathways of unconventional protein secretion. *Trends Cell Biol*. 2017;27:230–240.
43. Gee HY, Kim J, Lee MG. Unconventional secretion of transmembrane proteins. *Semin Cell Dev Biol*. 2018;83:59–66.
44. Dupont N, Jiang S, Pilli M, Ornatowski W, Bhattacharya D, Deretic V. Autophagy-based unconventional secretory pathway for extracellular delivery of IL-1β. *EMBO J*. 2011;30:4701–4711.
45. Ponpuak M, Mandell MA, Kimura T, Chauhan S, Cleyrat C, Deretic V. Secretory autophagy. *Curr Opin Cell Biol*. 2015;35:106–116.
46. Gonzalez CD, Resnik R, Vaccaro MI. Secretory autophagy and its relevance in metabolic and degenerative disease. *Front Endocrinol (Lausanne)*. 2020;11:266.
47. Buratta S, Tancini B, Sagini K, et al. Lysosomal exocytosis, exosome release and secretory autophagy: the autophagic- and endo-lysosomal systems go extracellular. *Int J Mol Sci*. 2020;21:2576.
48. Ganesan D, Cai Q. Understanding amphisomes. *Biochem J*. 2021;478:1959–1976.
49. Andrews NW. Regulated secretion of conventional lysosomes. *Trends Cell Biol*. 2000;10:316–321.
50. Jaiswal JK, Andrews NW, Simon SM. Membrane proximal lysosomes are the major vesicles responsible for calcium-dependent exocytosis in nonsecretory cells. *J Cell Biol*. 2002;159:625–635.
51. New J, Thomas SM. Autophagy-dependent secretion: mechanism, factors secreted, and disease implications. *Autophagy*. 2019;15:1682–1693.
52. Cho G, Bragiel AM, Wang D, et al. Activation of muscarinic receptors in rat parotid acinar cells induces AQP5 trafficking to nuclei and apical plasma membrane. *Biochim Biophys Acta*. 2015;1850:784–793.
53. Reczek D, Schwake M, Schröder J, et al. LIMP-2 is a receptor for lysosomal mannose-6-phosphate-independent targeting of β-glucocerebrosidase. *Cell*. 2007;131:770–783.
54. Brennan LA, Kantorow WL, Chauss D, et al. Spatial expression patterns of autophagy genes in the eye lens and induction of autophagy in lens cells. *Mol Vis*. 2012;18:1773–1786.
55. Cleyrat C, Darehshouri A, Steinkamp MP, et al. Mpl traffics to the cell surface through conventional and unconventional routes. *Traffic*. 2014;15:961–982.
56. Griffiths RE, Kupzig S, Cogan N, et al. Maturing reticulocytes internalize plasma membrane in glycophorin A-containing vesicles that fuse with autophagosomes before exocytosis. *Blood*. 2012;119:6296–6306.
57. Ishikawa Y, Iida H, Ishida H. The muscarinic acetylcholine receptor-stimulated increase in aquaporin-5 levels in the apical plasma membrane in rat parotid acinar cells is coupled with activation of nitric oxide/cGMP signal transduction. *Mol Pharmacol*. 2002;61:1423–1434.
58. Ishikawa Y, Yuan Z, Inoue N, et al. Identification of AQP5 in lipid rafts and its translocation to apical membranes by activation of M3 mAChRs in interlobular ducts of rat parotid gland. *Am J Physiol Cell Physiol*. 2005;289:C1303–C1311.
59. Kosugi-Tanaka C, Li X, Yao C, Akamatsu T, Kanamori N, Hosoi K. Protein kinase A-regulated membrane trafficking of a green fluorescent protein-aquaporin 5 chimera in MDCK cells. *Biochim Biophys Acta*. 2006;1763:337–344.
60. Kitchen P, Öberg F, Sjöhamn J, et al. Plasma membrane abundance of human aquaporin 5 is dynamically regulated by multiple pathways. *PLoS One*. 2015;10:e0143027.
61. Sidhaye VK, Güler AD, Schweitzer KS, D'Alessio F, Caterina MJ, King LS. Transient receptor potential vanilloid 4 regulates aquaporin-5 abundance under hypotonic conditions. *Proc Natl Acad Sci USA*. 2006;103:4747–4752.
62. Liu X, Bandyopadhyay BC, Nakamoto T, et al. A role for AQP5 in activation of TRPV4 by hypotonicity: concerted involvement of AQP5 and TRPV4 in regulation of cell volume recovery. *J Biol Chem*. 2006;281:15485–15495.
63. Calamita G, Ferri D, Gena P, et al. The inner mitochondrial membrane has aquaporin-8 water channels and is highly permeable to water. *J Biol Chem*. 2005;280:17149–17153.
64. Amiryl-Moghaddam M, Lindland H, Zelenin S, et al. Brain mitochondria contain aquaporin water channels: evidence for the expression of a short AQP9 isoform in the inner mitochondrial membrane. *FASEB J*. 2005;19:1459–1467.
65. Liu Y, Fiskum G, Schubert D. Generation of reactive oxygen species by the mitochondrial electron transport chain. *J Neurochem*. 2002;80:780–787.
66. Marchissio MJ, Francés DEA, Carnovale CE, Marinelli RA. Mitochondrial aquaporin-8 knockdown in human hepatoma HepG2 cells causes ROS-induced mitochondrial depolarization and loss of viability. *Toxicol Appl Pharmacol*. 2012;264:246–254.

Investigative Ophthalmology & Visual Science

67. Watanabe S, Moniaga CS, Nielsen S, Hara-Chikuma M. Aquaporin-9 facilitates membrane transport of hydrogen peroxide in mammalian cells. *Biochem Biophys Res Commun*. 2016;471:191–197.
68. Krüger C, Jörns A, Kaynert J, et al. The importance of aquaporin-8 for cytokine-mediated toxicity in rat insulin-producing cells. *Free Radic Biol Med*. 2021;174:135–143.
69. Hayashi R, Hayashi S, Fukuda K, Sakai M, Machida S. Immunolocation of aquaporin 8 in human cataractous lenticular epithelial cells. *Biomed Hub*. 2017;2:1–5.
70. Rodrigues C, Pimpão C, Mósca AF, et al. Human aquaporin-5 facilitates hydrogen peroxide and cancer cell migration. *Cancers (Basel)*. 2019;11:932.
71. Lee J, Giordano S, Zhang J. Autophagy, mitochondria and oxidative stress: cross-talk and redox signalling. *Biochem J*. 2012;441:523–540.
72. Scherz-Shouval R, et al. Reactive oxygen species are essential for autophagy and specifically regulate the activity of Atg4. *EMBO J*. 2007;26:1749–1760.